DARK AND LUMINOUS MATTER IN SPIRAL GALAXIES

Thesis submitted for the degree of
"Doctor philosophiae"

CANDIDATE
Paolo Salucci

SUPERVISOR
D.W. Sciama

December 1986

AKNOWLEDGMENTS

It is a pleasure to thank my supervisor Dennis Sciama for giving me an interesting and very promising reseach field and the working idea of a dynamical evolution leading to the present properties of spiral.

I would like to thank him also for his continuous guidance and encouragement during these past three years.

I have benefitted enormously from the many dicussions with V. Rubin and G. Chincarini on the observational side of problems, that I and/or my collaborator M. Persic had.

I am also grateful to Gianfranco De Zotti, Maria Petrou , Fernando de Felice and Luigi Danese for many long and useful conversations and Maria P. for her warm hospitality in Oxford.

The work on the phenomenological properties of galaxies and the test for alternatives to dark matter were done in friendly collaboration with Massimo Persic and Mark Dubal, respectively.

I would like to thank C. Chiosi for several discussions on evolutionary models and G. Bertin for useful comments on the first Chapter.

Finally, I am very pleased to thank people at SISSA that during these three years encouraged my work and created a very stimulating atmosphere .

INDEX

GENERAL INTRODUCTION

At the present, in trying to understand the Universe, spiral galaxies are one of the most exciting research fields, both for astronomers and theoretical physicists. In fact, they are the final product of the process that from an homogeneous medium develops the very small inhomogeneities present, whish in turn form bound systems of 10^9-10^{12} solar masses. On the other side, spirals are real laboratories in which unknown particles (or unknown objects) have been largely and unequivocably detected. Moreover a spiral galaxy is the place where stars form and are organized and displayed in beautiful patterns.

Even a simple inspection of the observational scenario undoubtedly calls for new physics and/or new astrophysics to a large extent. It is important to realize that this happens in galaxies of very different integral properties (masses range from 10^9 to 10^{12} solar masses) and optical appearances (in any Hubble type from S0 to Sdm) and independently of individual peculiarities such as bars, companions, strong bulges, hydrogen content deficiency, starbusts.

Nevertheless, despite this overwhelming evidence a satisfactory theoretical scenario have not been developed yet. In particular many crucial questions, raised both by observations and theoretical investigations, still demand a univoque and quantitative answer:

1) Is the dark matter, surely present in many galaxies, present in all galaxies ?

2) Is the dark matter dynamically relevant within the optical disk ?

3) What is the Nature of dark matter ?

4) What were the properties of the dark proto-halo ?

5) How is the disk formed ?

6) How has visible matter acquired its angular momentum. ?

7) Why dark matter seems to couple with visible matter in

driving integral properties of galaxies ?

8) Where does the Hubble sequence comes from ?

I want to stress that these questions basically reflect our ignorance on **what** the integral and local properties of spiral galaxies are rather than on **where** they come from.

In fact, if we look carefully at the present status, both observational and theoretical of late stages of galaxy formation and present structure, we realize that, although some physical processes still need to be understood and more observations would be welcomed, the more serious problems come from the fact that we have not the **model** of a spiral galaxy nor those of a proto-halo on which to study the physics of processes and by means of which interpret observations in order to draw the underlying physics.

I would like to point out that this is not surprising: in fact, actually in spiral galaxies we do not see what is known and we do know what is seen.

On the other hand we have a lot of empirical correlations linking each other, practically any observable galaxy property, and whose physical meaning often is not very clear. Nevertheless, I feel that this is a very important point that is disregarded in the literature: theories should pay more attention to the present status of galaxies that is much more complex with respect to the idealized one and involves a large range in their integral properties such as some amazing regularity found in very different galaxies.

So, the aim of this thesis is to build up a working model, derive from the observational quantities the physically relevant ones and understand how the new astro(physics) works in galaxies.

In order to reach this goal it is very crucial to use a suitable strategy in dealing with observations and theory. In detail:

1) I fix on general properties and on recurring unexplained facts.

2) I work out a model-independent investigation in order to

organize the observable properties of galaxies and build up a phenomenological scenario for spirals.
3) Therefore, the physically relevant properties are obtained by matching a minimal assumptions model with this model-independent scenario.

So, I neglect any occasional peculiarity, and investigate quantitatively individual differences of general features.

After I have discussed the motivations and purposes of this Thesis, I explain how it is organized.

In the first Chapter I draw a phenomelogical scenario for spirals: much information on local and global properties is stored in the rotation curves and can be recovered by realizing that individual differences of total (dark + visible) integral quantities are imprinted on the profiles of rotation curves.

Moreover, some recurrent feature involved with the slope of rotation curves show phenomenologically the existence of a connection between the dark component and the visible one. Taking into account this I can give a phenomenological support to the empirical relations (i.e. Tully-Fisher relations) found in spirals.

Quite a lot of theoretical effort has been done towards alternatives to dark matter involving modifications of Newtonian gravity law. From the results of the previous Chapter, we find that these theories are easily testable by comparing their predictions with the developed observational scenario. Therefore, we think that it is worthwhile, before proceeding further in the dark matter scenario, to investigate how realistic is the possibility that such modifications of fundamental physical laws originate the mass discrepancies we observe in spirals. Then, in Chapter 2 I show that, although we cannot exclude a priori any alternative to dark matter, nevertheless the proposed modifications are very far from fitting observations.

In the chapter 3 halo and disk fundamental integral

properties are worked out: firstwhole I follow a model-independent approach to them able to describe phenomenologically the link between the observable quantities with the physically relevant ones. Then, the minimal assumptions model that I am going to use is carefully analyzed and checked. Finally, by means of a method that minimize the effects of our poor knowledge of local properties of dark halos and by using the whole observational scenario developed in the first Chapter ,the integral properties for disks and halos are worked out. These are in perfect agreement with those obtained by an empirical, but model independent, approach.

We want to explain how the 3 appendices are conceived in the structure of this work: they are not the detailed proof of some partial and auxiliary result but instead they are used to show results whose importance even exceeds that which might be inferred by the role that they have throughout this work. In fact, in Appendix 1 we phenomenologically show in detail that with respect to many aspects relevant to the axisymmetric structure so as the non-axysimmetric one, spirals form an one-parameter sequence , in appendix B links between axisymmetric structure and spiral structure are found out; in Appendix C we discuss how to obtain the circular velocity from the observational data and we give examples of serious troubles arising from incorrect methods.

CHAPTER 1

THE INFORMATION ON LARGE-SCALE PROPERTIES OF SPIRAL GALAXIES STORED IN THEIR KINEMATICS

INTRODUCTION

The rotation curves of spiral provide good evidence for the presence of large amounts of unseen (dark) matter. (Faber and Gallagher, 1979; Rubin, Ford, Thonnard 1980; 1982; 1986; Chincarini and de Sousa, 1985 Burstein and Rubin, 1986; Carignan and Freeman, 1986 ; van Albada and Sancisi, 1986, in the next Chapter we address quantitatively this topic).

In agreement with the generally accepted scenario of galaxy formation , observational data indicate that baryonic matter is mostly situated within a thin disk which is surrounded by a dark halo. Nevertheless, rotation curves do not show any kinematical trace of the individual dark and visible components. Moreover, the transition zone between a disk-dominated and a halo-dominated region, which is naturally expected in this two-component model seems to have been smoothed out. It is reasonable to believe that in the late stages of the collapse some mass and angular momentum redistribution occurred which destroyed the relevant features in the rotation curves (probably via non axi-symmetric perturbations (Sciama, 1984)).

It is important to realize that spiral galaxies span over two order of magnitudes in their integral properties and greatly differ in the development of spiral structure, but nevertheless the individuality of each galaxy in not manifested by some gross difference in their circular velocity fields. A question then arises: to what extent do the observed rotation curves, which are devoided of any striking features, carry information on the integral properties of spiral galaxies ?

The aim of this Chapter is to show the the amount of information which can be obtained from the kinematics can be enlarged by a deep investigation of the circular velocity fields

and their gradients. To this purpose it is useful to study the quantity $\tilde{V} \equiv (\Omega - \varkappa/2)\, R$, where $\Omega(R)$ is the angular velocity and $\varkappa(R)$ is the epicyclic frequency. This quantity essentially "represents" the gradients of the circular velocity $V(R) = \Omega R$ and of many local quantities (see Appendix A).

$\tilde{V}$ turns out to be practically constant out to large radii even for galaxies with steep rotation curves, being its radial variation, typically 5-10 times smaller than those of the circular velocity (Note that this property of spiral galaxies might remind us of Lindblad's old suggestion (Lindblad, 1956) that the quantity $\Omega_L = \Omega - \varkappa/2$ is constant in our Galaxy and as such it plays a crucial role in the formation of spiral structures. In this Chapter, however, We shall study the phenomenological large-scale importance of the distance-independent quantity $\tilde{V} \equiv \Omega_L R$).

In addition, $\tilde{V}$ is strongly connected with the prominence of spiral structure (see Appendix B) and with local and large scale properties. This arises from the fact that the range of circular velocity among galaxy is much smaller than the range of circular velocity gradients.

The main sample of galaxies which we have used to investigate this connection, hereafter sample A, comes from Rubin et. al. (1982, 1984); moreover, the results found for sample A have been checked in a bigger sample, hereafter Sample B, which contains virtually all the extended high quality rotation curves which are readily available in the literature.

The results of this Chapter suggest the the gradient of the circular velocity (or equivalently $\tilde{V}$) is a model-independent basic quantity suitable for extending our knowledge of spiral galaxies. In fact $\tilde{V}$ is found to be the most relevant quantity in describing many individual aspects of the theoretical framework pertinent to spiral galaxies and can be used to throw light on the luminosity/kinematics coupling through Tully-Fisher-like relations linking $\tilde{V}$ to absolute magnitudes and optical sizes.

The plan of this chapter is the following: in section I , we demonstrate the constancy of $\tilde{V}$; in section II , we propose $\tilde{V}$ as a good indicator of galactic magnitudes and sizes; in section III , we analyze the previous results and work out a simple regularity shared by kinematical bisymmetric perturbations in all the spiral galaxies in our sample.

I THE CONSTANCY OF $\tilde{V}$

Let $\phi(R)$ be the axisymmetric gravitational potential in the plane of the galaxy disk, so

$$V^2 = R\, d\phi/dr \qquad (I.1)$$

gives the circular velocity. We define

$$\tilde{V} \equiv (\Omega - \varkappa/2)\, R \qquad (I.2)$$

where $\varkappa(R)$ is the epicyclic frequency, given by:

$$\varkappa^2 = R^{-3}\, d/dr\, (V^2R^2) \qquad (I.3)$$

To obtain the circular velocity V from the observational data V_{obs} we are forced to take into account (see appendix C) the general property of spiral galaxies the the gradient of the circular velocity does not vary on a scale large than the interarm spacing, i.e. V(R) varies on a linear scale (Rubin et. al. 1980, 1982, 1985) . Thus, by means of a linear least square fit we get:

$$V(R) = V_0 + V_1\, (R/R_{25}) \qquad R \geq R_B \qquad (I.4)$$

where V_0 and V_1 are the coefficients of the fit (Table 1), R_B is the smallest radius from which outwards the rotation curves takes

a linear behaviour and R_{25} is the 25 mag arsec^{-2} contour. R_B is easily found in all galaxies, typically $R_B/R_{25} \leq 0.1\text{-}0.3$. Then from (I.2) - (I.4) we compute $\tilde{V}(R)$ for the galaxies of the sample: **the radial variations I found are always very small** (a few percent at the most, see figure 1).

It is important make us sure that neither the constancy of $\tilde{V}$ nor its value depend upon any reasonable choice of R_B: the maximum variations of the value of $\tilde{V}$ with R_B are always small (10% - 20%) and its constancy it is independent of R_B. Nevertheless, in a few galaxies of the sample the presence of quit strong non-circular motions cause some uncertainties in deriving the values of the velocity gradient and therefore in the value of $\tilde{V}$: an extreme case is NGC 1357 for which the data are unable to give the large scale behaviour of circular velocity and therefore was left out of sample A.

We can easily realize that the radial variation of $\tilde{V}$ are remarkably smaller than those of the circular velocity regardless of the slope of this latter: in fact by setting $x = V_1/V_o$, so that $(d\log V/d\log R)_{25} = x/(1+x)$ (with typically $-0.2 \leq x \leq 1$), we have:

$$\left| d\tilde{V}/\tilde{V} \right| \leq (1-\sqrt{2})^{-1} \left| (1+x)\left[1 - 1/\sqrt{2}(1+x/(1+x))^{-1/2}\right] - 1 \right| \qquad (I.5)$$

where $| d\tilde{V}/\tilde{V} |$ is the percentage variation of $\tilde{V}$ over the whole disk. From (I.5) we have that $| d\tilde{V}/V |$ is very small even for steep rotation curves: $| d\tilde{V}/\tilde{V} |_{x=1} \leq 0.1$ and $| (d\tilde{V}/\tilde{V})/(dV/V) |$ is typically ~ 0.1 .

As an interesting consequence of (I.5) we have $\Omega_L \propto 1/R$. This implies that the widely accepted constancy of this quantity (see e.g. Dekker, 1977; Bertin, 1981; Fridman and Polyachencko, 1984; Athanassoula, 1985) is not observationally supported being large its variation along the whole disk:

$$(\Omega_L(R_B) - \Omega_L(R_{25}))/\Omega_L(R_{25}) = (R_{25}/R_B - 1) \simeq 2\text{-}5 .$$

To conclude this section we wish to stress that the constancy of $\tilde{V}$ (or equivalently the constancy of the gradient of the circular velocity over a large portion of the stellar disk) reflects the fact that spiral galaxies do not show in the rotation curves any transition between a disk-dominated and a halo-dominated region. Thus the spherical distribution of dark matter seems to be related to the disk distribution of visible matter in that both act in agreement to make $\tilde{V}$ constant over the whole disk in galaxies of very different scale properties (mass and size).

II. $\tilde{V}$ AS AN INDICATOR OF LUMINOSITIES AND SIZES

The coupling between kinematics and luminosity for galaxies has been widely expressed in terms of relations between a reference velocity and blue (infrared) magnitude (or isophotal radius) (Tully and Fisher, 1977; Aaronson et. al. 1979; see also Richter and Huchtmeier, 1984 and references therein ; the whole sample A is widely studied in Rubin et. al., 1985: this is why we keep in this sample a few galaxies whose rotation curve is not sufficiently extended). These empirical relations, in addition to giving a promising method of obtaining the Hubble constant and the shape of our supercluster , enable one to compare the distribution of luminosities with the distribution of masses in galaxies of very different integral properties and Hubble types.

Nevertheless , the Tully-Fisher relation (hereafter TF) gives rise to a number of unsolved problems: (1) a fairly large intrinsic scatter, (2) a troublesome Hubble-type dependence of the zero-point and above all (3) no physical explanation of their origin beyond the very general idea that both luminosity and circular velocity might be different "measures" of the same mass.

In this context we think that it is worthwhile to bring the circular velocity gradient (or equivalently $\tilde{V}$) into the discussion

so that we may explore the luminosity/kinematics coupling from a different point of view. Accordingly, in this section we search for empirical relations between $\tilde{V}$ and the integral quantities such as luminosity and isophotal radius. In doing so we are encouraged by the three following facts:

a) $\tilde{V}$ "governs" many important local quantities in particular the effective total density (see Appendix A)

b) $\tilde{V}$ has a unique value throughout the disk, so that one avoids the problem of choosing the best reference value.

c) $\tilde{V}$ in addition to being in each galaxy sensitive to the gradient of the circular velocity, turns out a "measure" , in statistical sense, of the circular velocity. In fact, we find a strong connection between $\tilde{V}$ and any reference velocity. For sample A we have:

$$\log \tilde{V} = -(2.6\pm0.3) + (1.8\pm0.1) \log V_M \qquad \text{(I.7)}$$
$$42 \text{ Sb-Sc} \qquad r = 0.89$$

with V_M the maximum circular velocity and r the correlation parameter of the linear regression. Equation (I.7) is the quantitative counterpart of the observational evidence that smaller galaxies tend to have steeper rotation curves (Rubin et.al., 1980): smaller galaxies have smaller circular velocities and then from (I.7) , lower values of the ratio $\tilde{V}/V_M$ which in turn imply (see (I.2) and (I.3)) higher gradients of circular velocity.

For sample A, we obtain (see figures 2a, 2b):

$$M_B = (-12.7\pm1.6) - (5.1\pm0.9) \log \tilde{V}$$
$$22 \text{ Sb} \qquad r = 0.77 \qquad \sigma = 0.62 \text{ mag}$$

(I.8)

$$M_B = (-15.0\pm1.0) - (4.2\pm0.7) \log \tilde{V}$$
$$20 \text{ Sc} \qquad r = 0.82 \qquad \sigma = 0.64 \text{ mag}$$

where M_B is the absolute blue magnitude, σ is the scatter and $\tilde{V}$ is expressed in km s^{-1}.

We shall now investigate the mutual statistical dependence among the TF , the $M_B/\tilde{V}$, and the $\tilde{V}/V_M$ relations. To this end we use the Spearman rank correlation to test the null hypothesis that each of these relations arises entirely from the other two. The crucial quantity that is worked out by applying this test is the significance level $D_{xy,z}$ of the x/y relation , obtained after considering also the existence of the x/z , and y/z relations.

The results of this test (see Table 2) indicate that:

a) $\tilde{V}$ is a new luminosity indicator in spite of the existence of a tight $\tilde{V}/V_M$ relation, that is the $M_B/\tilde{V}$ relation **does not depend on the existence of TF relation.**

b) The relation between circular velocity and its gradient turns out the highest (empirical) relation found in spirals so that it seems crucial to understand it do draw a satisfactory picture of the present structure of spiral galaxies. Note that this relation is not absolutely expected in the disk/halo scenario: its existence involves a strong connection between the dark component and the visible one.

Upon a comparison in the same sample of (I.8) with the TF (Rubin et. al., 1985), we note that the former seems to be less dependent on the morphological type (see Table 3). This is also reflected by the fact that grouping together all the 42 galaxies we still get a good correlation:

Upon a comparison in the same sample of (I.8) with the TF (Rubin et. al., 1985), we note that the former seems to be less dependent on the morphological type (see Table 3). This is also reflected by the fact that grouping together all the 42 galaxies we still get a good correlation:

$$M_B = (-15.6\pm0.8) - (3.6\pm0.5) \log \tilde{V} \qquad \text{(I.9)}$$

42 Sb+Sc $r = 0.74$ $\sigma = 0.70$ mag

Note that for the same sample:

$$M_B = (-1.2\pm2.6) - (8.8\pm1.1) \log V_M \qquad \text{(I.10)}$$

42 Sb+Sc $r = 0.68$ $\sigma = 0.77$ mag

and performing again the Spearman test we have:

$$D_{M_B V_M,\tilde{V}} = 0.2 \quad , D_{M_B \tilde{V},V_M} = 3.3 \quad , D_{\tilde{V}V_M,M_B} = 5.9$$

Thus we are led to the conclusion that, at least for a morphologically mixed sample, the M_B/V_M relation is induced by the $\tilde{V}/V_M$ relation from the $M_B/\tilde{V}$ one.

Although we found again the result (Rubin et. al., 1985) that the luminosity/kinematics relation has a zero/point dependent on the Hubble type, nevertheless, when the velocity gradients are taken into account , this morphological dependence is remarkably reduced (see Table 3).

Sample A is not free from selection effects; for instance it has been selectionated with the intention of spanning a range as large as possible in integral galaxy properties (luminosities, radii): this procedure gives too much statistical importance to rare individuals; moreover other selective biases can be easily worked out. Then, in order to enlarge the sample and investigate/eliminate possible selection effects, we shall study a bigger sample (hereafter Sample B) including sample A , without NGC 7217 reported in RC2 as a Sa and NGC 4800 whose inclination is quite uncertain, and all Sb-Sc galaxies found in the literature and having:

a) an extended rotation curve: $R_f/R_{25} \geq 0.7$, with R_f the farthest radius with measured circular velocity.

b) radial corrected heliocentric motion ≥ 1000 km s^{-1} to prevent large peculiar velocity from affecting the determination of distances. Unfortunately this threshold is rather low because of the small number of suitable galaxies found at higher redshifts

c) no large non-circular motions

d) low internal scatter for the measured rotational velocity at a given galactocentric radius:

e) for curves obtained from radio observations R_{25}/(beam size) > 2.

We have found the galaxies NGC 4565, NGC 5383, NGC 7331, NGC 5033, (Bosma, 1981); NGC 1085 (Barabanov et al. , 1981); NGC 5426 (Blackman, 1982); NGC 3992 (Gottesman, 1984); NGC 7339 (Kyazumov, 1980); NGC 2336, NGC 5290, NGC 5905, I65, I 1090, (van Moorsel, 1984); NGC 2870, NGC 3526 (Karachenchev et al. , 1984); NGC 4254, NGC 4654, (Chincarini and de Sousa, 1985); NGC 5673 (Morris et al. , 1985), which meet the requirements a) - e).

After their magnitudes and radii have been corrected according to Rubin et al.(1982), this enlarged sample, ∿ 40 % more objects, can be used to rule out the possibility that selection effects strongly bias the results obtained for sample A. In fact sample B turns out to be statistically indistinguishable from sample A (see also figure 3):

$$M_B = (-15.2\pm0.7) - (3.9\pm0.4) \log \tilde{V} \qquad \text{(I.11)}$$
$$59 \text{ Sb+Sc } r = 0.79 \quad \sigma = 0.60 \text{ mag}$$

For this sample the scatter of TF relation is 0.73 mag; this result shows that a considerable fraction of TF arises from gradient effects, that is from differences of density distribution and/or total amount of the dark matter along the luminosity sequence or in galaxies having the same total mass. (note that at this point we cannot discriminate between these two possibilities without a model. However, we want anticipate that in next Chapter we shall find that the latter is the actual one.)

Then, we can work out the explicit relation between the isophotal radius R_{25} and $\tilde{V}$:

$$\log R_{25} = (-0.29\pm0.41) + (0.99+0.24) \log \tilde{V}$$
20 Sb $\qquad r = 0.70$

(I.12)

$$\log R_{25} = (-0.22\pm0.22) + (1.00\pm0.15) \log \tilde{V}$$
22 Sc $\qquad r = 0.85$

where R_{25} is expressed in kpc.

Grouping together all Sb and Sc galaxies, we get for sample A.

$$\log R_{25} = (-0.10\pm0.17) + (0.9\pm0.1) \log \tilde{V} \qquad \text{(I.13)}$$
$$40 \text{ Sb+Sc} \quad r = 0.77 \quad \sigma = 0.62 \text{ mag}$$

and for sample B (see figure 4):

$$\log R_{25} = (-0.15\pm0.17) + (0.92\pm0.1) \log \tilde{V} \qquad \text{(I.14)}$$
$$22 \text{ Sb} \quad r = 0.77 \quad \sigma = 0.62 \text{ mag}$$

A useful consequence of the tightness of the $R_{25}/\tilde{V}$ relation is that we can obtain a good estimate of the typical effective galactic density $\rho_{25} = \rho(R_{25})$ as defined in A1, in that ρ_{25} varies among galaxies mainly as function of R_{25}:

$$\log \rho_{25} = (-0.4\pm0.4) - (1.4\pm0.2) \log \tilde{V} \qquad \text{(I.15)}$$
$$59 \text{ Sb+Sc} \quad r = 0.62$$

Then, smaller galaxies are the denser ones. It is important to note that a relation analogous to (I.15) involving the circular velocity is found to show a very poor correlation; this can be explained by realizing that ρ_{25} depends mainly on the amount of dark matter inside and its distribution at R_{25}, whereas V_M weighs the total mass inside R_{25}.

A crucial issue of the TF relations is their possible band-dependence: it is well known that infrared magnitudes represent the old disk population (responsible for most of stellar mass) better than blue magnitudes (Aaronson et al., 1979). Nevertheless, a detailed comparison of the results obtained in different bands needs a large statistical sample, so that the relation found with the presently available data (collected in Whitmore, 1984) should be considered as preliminary:

$$M_H = (-14.8\pm2.0) - (5.4\pm1.2) \log \tilde{V} \qquad \text{(I.16)}$$

17 Sb $\quad r = 0.78 \quad \sigma = 0.60$ mag

$$M_H = (-15.9 \pm 1.2) - (4.9 \pm 0.8) \log \tilde{V} \qquad \text{(I.17)}$$

19 Sb $\quad r = 0.83 \quad \sigma = 0.70$ mag

$$M_H = (-16.1 \pm 0.9) - (4.7 \pm 0.5) \log \tilde{V} \qquad \text{(I.18)}$$

36 Sb+Sc $\quad r = 0.83 \quad \sigma = 0.67$ mag

These relations. when compared to their analogous (I.8) and (I.9) in the blue band, seems to indicate a lesser dependence on the morphological type (see Table 3), well in agreement with the fact that a fraction of the blue luminosity arises from components whose importance varies along the Hubble sequence.

We can summarize the results of this section by saying that when "gradients effects" are taken into account, that is to phenomenologically include possible differences in the dark component among galaxies which affect directly the profile of the rotation curve, then we can both improve the TF relations and also to link local properties of spiral galaxies to their integral ones.

III A COMMON PROPERTY OF SPIRAL GALAXIES

An important consequence of the $R_{25}/\tilde{V}$ relation is that the frequency $\tilde{\Omega}_D \equiv (\Omega - \varkappa/2)_{R_{25}}$ has practically the same value in all galaxies in spite of the fact that their scale properties vary by two orders of magnitudes. In fact from (I.12) we have:

$$R_{25} \propto \tilde{V} \propto \tilde{\Omega}_D \, R_{25} \qquad \text{(I.19)}$$

In addition to this general trend we obtain for sample B:

$$\langle \tilde{\Omega}_D \rangle = 2.0 \pm 0.7 \qquad \text{(I.20)}$$

in units of km $s^{-1}kpc^{-1}$, where the reported error is the 1-σ uncertainty.

$\tilde{\Omega}_D$ is a remarkable regularity and could provide hints and constraints to theories aimed to explain the formation of the disk and its acquisition of angular momentum.

Moreover, this regularity actually extends to any radius $R > R_B$ within the stellar disk. In fact, from (I.2) and (I.19) we have:

$$\{ \Omega(R/R_{25}) - \varkappa(R/R_{25})/2 \} \simeq 2\ (R/R_{25})^{-1} \qquad \text{(I.21)}$$

where the units are km s^{-1} kpc^{-1}.

This result has an impact also on spiral structure theory: in fact, in view of the physical meaning of $\Omega - \varkappa/2$, that is the angular velocity of the slowest bisymmetric perturbance (see Toomre, 1977), expression (I.21) implies:

a) this frequency is practically the same at any R/R_{25} in each galaxy.

b) accordingly to QSSS theory the frequency Ω_p at which the spiral pattern rotates scales among spiral galaxies as R_{25}/R_i where R_i is the Inner Linblad Resonance.

We want to stress that a) and b) are the realization of (I.21) in some specific spiral structure scenario, nevertheless it is important to note that this relation is a model-independent property of spirals which constrains any theory of spiral structure.

IV SUMMARY AND CONCLUSIONS

In this Chapter we have shown that by taking into account the presence of a gradient of the circular velocity field we can significantly increase the amount of information on local and global properties of spiral galaxies available from kinematics. In fact by means of the "gradient" $\tilde{V}$ We found out two luminosity/kinematics relations analogous to the TF ones but carrying smaller intrinsic scatter and significantly lesser dependence on Hubble type: $L_B \propto \tilde{V}^{-1.5}$, $R_{25} \propto \tilde{V}$.

Furthermore, as consequence of the tightness of these relations we can obtain from the velocity field a good estimate of the effective density ρ_{25} of a spiral galaxy: $\rho_{25} \simeq 2\ 10^{-3}\ (\tilde{V}/50)^{-1.4}\ (M_\odot/pc^{-3})$.

These results indicate that circular velocity gradients (or equivalently $\tilde{V}$ should be profoundly involved in the scenario describing the latest stages of galaxy formation and in the present structure of galaxies as well. In fact, **in spite of the fact that spirals have two distinct mass components, their integral properties form an one-parameter sequence being the slope of the rotation curve the relevant parameter.**

Furthermore, 1) processes tending to make rotation curves flat such as outward transport of angular momentum via non-axisymmetric dynamical disturbances (Sciama, 1984), have a harder task: they must force a constant $\tilde{V}$ under very different physical conditions for densities, masses and sizes 2) It is present a regularity shared by all spiral galaxies: the frequency $(\Omega(R_{25}) - \varkappa(R_{25})/2)$ shows a strikingly small scatter among galaxies whose scale in mass and in size vary by two orders of magnitude.

	$r_{M_B\tilde{V}} = 0.779$		$r_{M_B\tilde{V},V_M} = 0.552$		$D_{M_B\tilde{V},V_M} = 2.6$
Sbr	$r_{M_BV_M} = 0.660$		$r_{M_BV_M,\tilde{V}} = 0.040$		$D_{M_BV_M,\tilde{V}} = 0.2$
	$r_{V_M\tilde{V}} = 0.829$		$r_{V_M\tilde{V},M_B} = 0.668$		$D_{V_M\tilde{V},M_B} = 3.4$
	$r_{M_B\tilde{V}} = 0.820$		$r_{M_B\tilde{V},V_M} = 0.413$		$D_{M_B\tilde{V},V_M} = 1.8$
Sc	$r_{M_BV_M} = 0.811$		$r_{M_BV_M,\tilde{V}} = 0.365$		$D_{M_BV_M,\tilde{V}} = 1.5$
	$r_{V_M\tilde{V}} = 0.858$		$r_{V_M\tilde{V},M_B} = 0.576$		$D_{V_M\tilde{V},M_B} = 2.6$

TABLE 1

Rank correlation coefficients, r_{xy} is the Spearman correlation coefficient between the variables x and y, $r_{xy,z}$ is the partial rank correlation with respect to variable z, and $D_{xy,z}$ is the significance level of this partial correlation.

V	$\tilde{V}$	$\Delta(M_B-\tilde{V})$	Δ(TFB)	$\Delta(M_H-\tilde{V})$	Δ(TFH)
150	20.7	1.1	1.1	0.4	0.3
200	34.7	0.9	1.2	0.3	0.6
250	52.0	0.7	1.4	0.2	0.9

TABLE 2

Differences in magnitudes for galaxies with the same circular velocity V_{25} ,and same $\tilde{V}$ obtained from (I.9), but belonging to different morphological types, Sc and Sb respectively. In columnes (3) - (6) are shown differences in magnitudes found in TF relation and in the analogous involving $\tilde{V}$ arising by considering a galaxy as a Sc or a Sb. We considered both blue (B) and infrared magnitudes (H).

FIGURE CAPTIONS

Fig. 1 $\tilde{V}$ as function of radius for typical galaxies belonging to sample A.

Fig. 2 Correlation between the absolute blue magnitude M_B and $\tilde{V}$ for the 22 Sb galaxies (top) and the 20 Sc galaxies (bottom) of the sample A .

Fig. 3 Correlation between the absolute blue magnitude M_B and $\tilde{V}$ for sample B (top).

Fig. 4 Correlation between the isophotal radius R_{25} and $\tilde{V}$ for sample B (bottom)

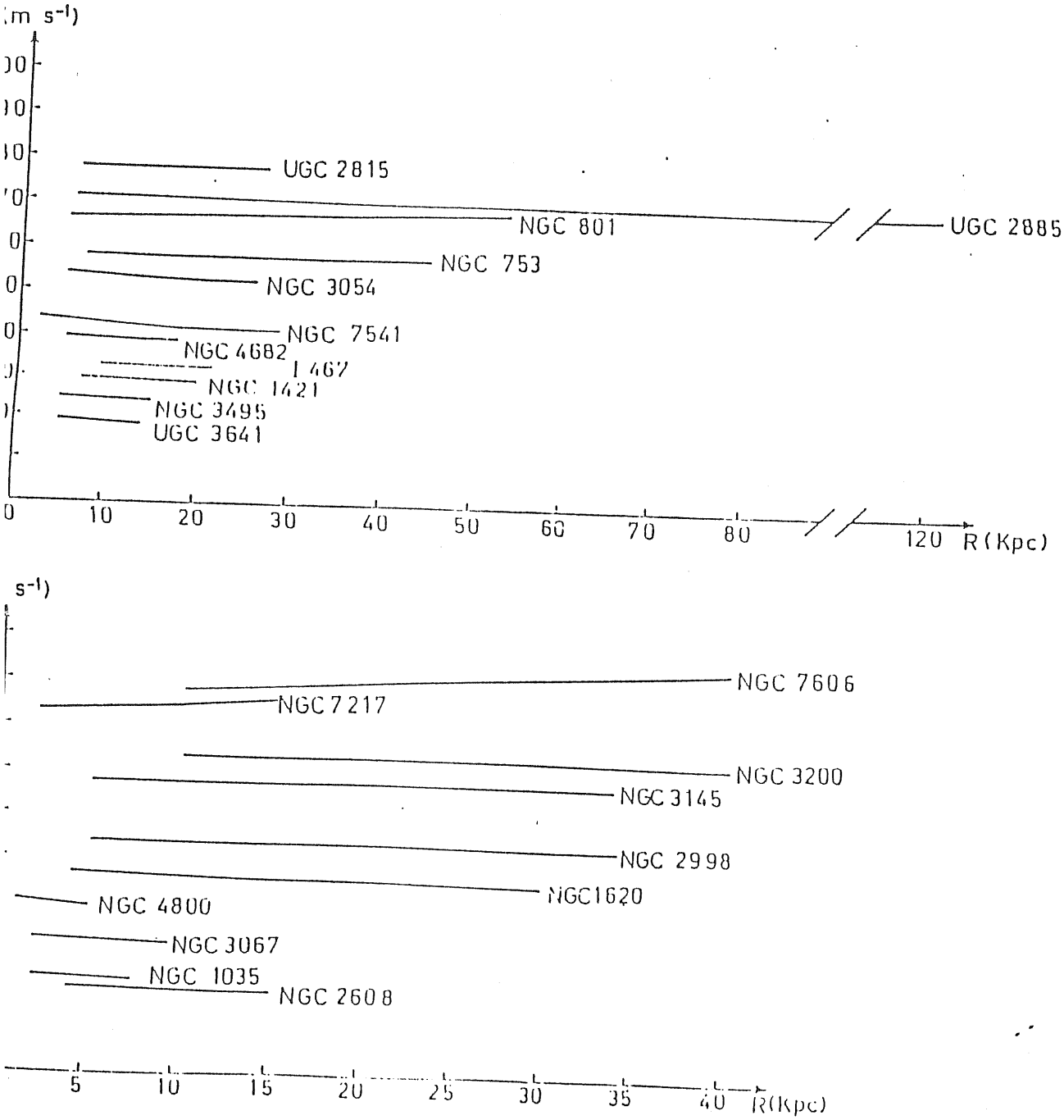
(m s⁻¹)
UGC 2815
NGC 801
UGC 2885
NGC 753
NGC 3054
NGC 7541
NGC 4682
I 467
NGC 1421
NGC 3495
UGC 3641
0
10
20
30
40
50
60
70
80
120
R (Kpc)

s⁻¹)
NGC 7606
NGC 7217
NGC 3200
NGC 3145
NGC 2998
NGC1620
NGC 4800
NGC 3067
NGC 1035
NGC 2608
5
10
15
20
25
30
35
40
R(Kpc)

FIGURE 1

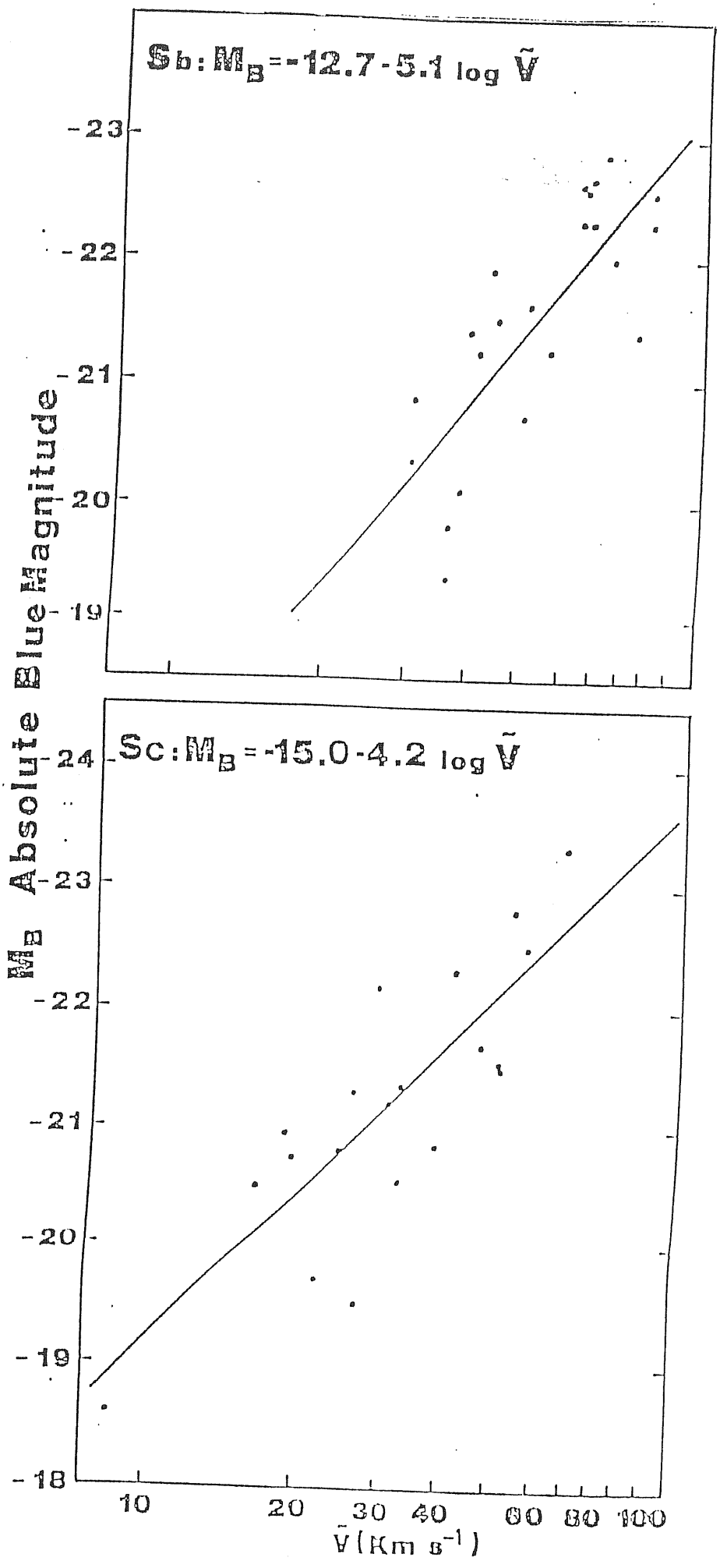
Sb: M_B = -12.7 - 5.1 log $\tilde{V}$
Sc: M_B = -15.0 - 4.2 log $\tilde{V}$
M_B Absolute Blue Magnitude
-23
-22
-21
-20
-19
-24
-18
10
20
30
40
60
80
100
$\tilde{V}$ (Km s^{-1})

FIGURE 2

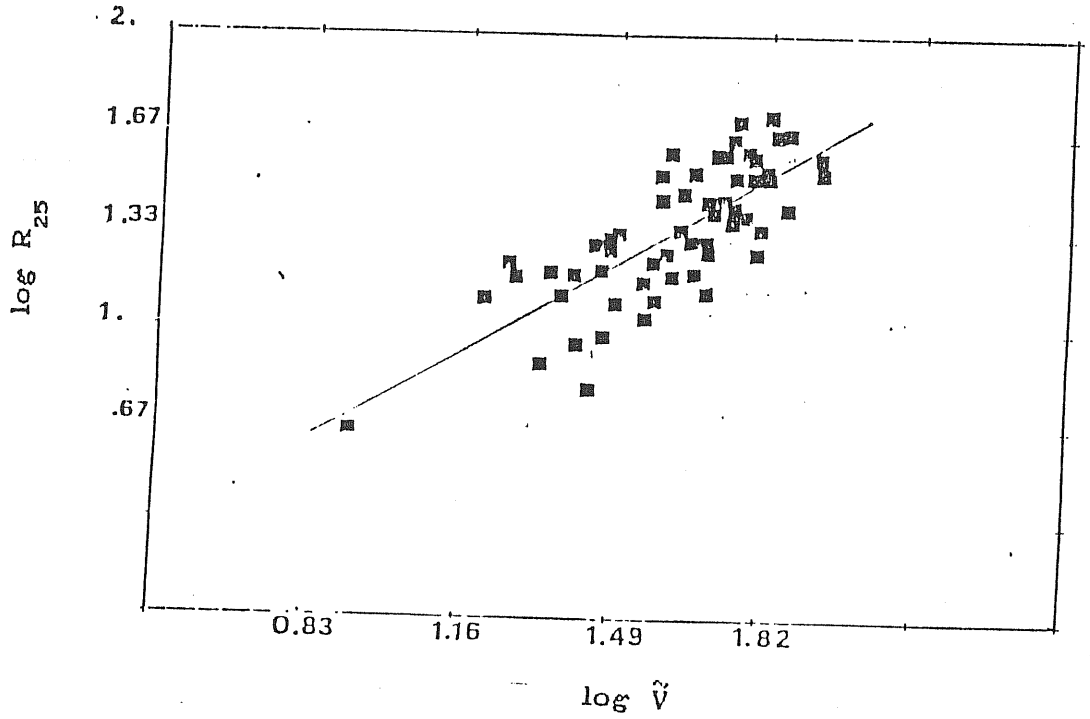

FIGURE 3

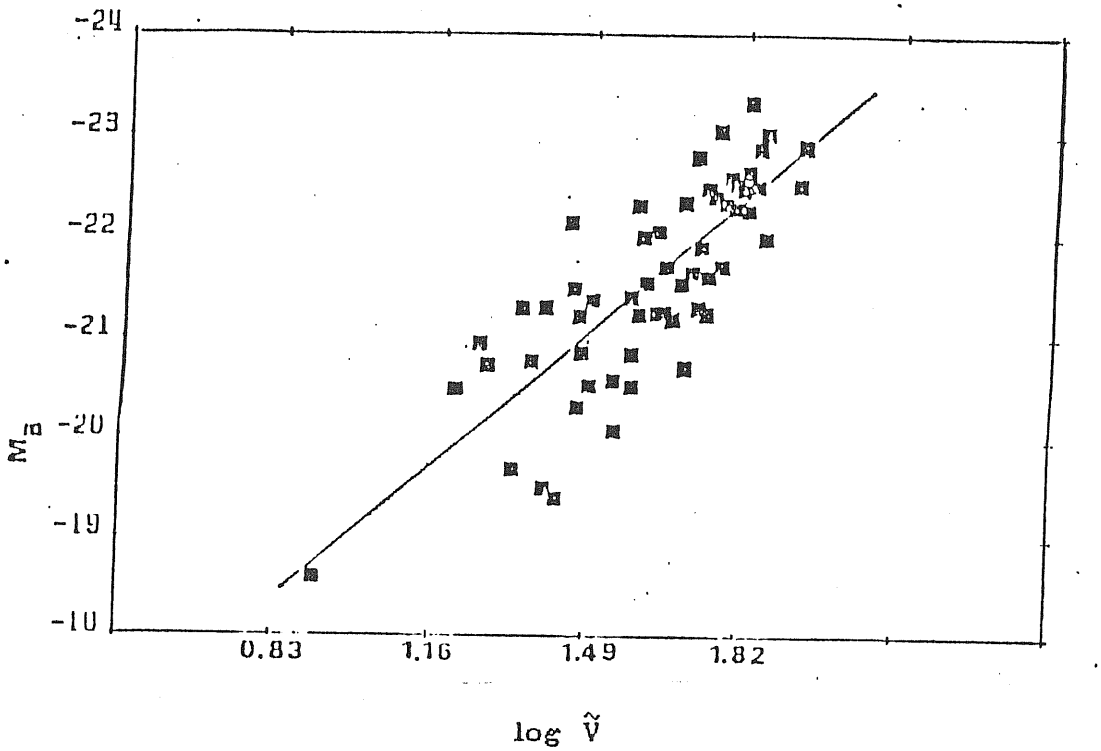

FIGURE 4

01

APPENDIX A

In this appendix we show some examples of how $\tilde{V}$ is naturally and usefully involved in the theoretical background of spiral galaxies, basically because the range of values of $\tilde{V}$ along the luminosity sequence is several times larger those of the circular velocity. Let us recall that $\tilde{V}$ is always constant over the whole disk outside the bulge, while the circular velocity can have moderate but significant increase.

I AXISYMMETRIC FRAMEWORK

a) in the external parts of the stellar disk, for which at a given radius R the amount of matter which resides in the disk exterior to R is negligible with respect to the total disk mass, i.e. according to the exponential thin disk model for $R > 2/3\ R_{25}$, a very good approximation for the total (disk + halo) mass $M(R)$ interior to R is: $M(R) \simeq 2\ 10^{-5}\ V^2 R$ with V expressed in km s^{-1} and R in kpc. Then, the local total density $\rho(R) = 1/(4\pi R^2)\ dM/dR$ takes the form:

$$\rho(R) = 1.8\ 10^{-5}\ V^2/R^2 \left\{ 3 - 8\ \eta + 4\ \eta^2 \right\} \qquad (A1)$$

where ρ is expressed in $M_\odot\ pc^{-3}$ and $\eta = \tilde{V}/V$.

b) epicyclic frequency $\varkappa(R)$

$$\varkappa = 2\ \Omega\ (1 - \eta) \qquad (A2)$$

c) Oort parameters A(R), B(R)

$$A = \Omega \left\{ 1 - (1 - \eta)^2 \right\}$$

$$B = - \Omega\ (1 - \eta)^2 \qquad (A3)$$

d) logarithmic gradient of angular velocity, circular velocity, specific angular momentum J, kinetic energy T, and of total mass M, see (A1):

$$\frac{d\ln \Omega}{d\ln R} = 2\,(1-\eta)^2 - 1$$

$$\frac{d\ln \Omega}{d\ln R} = \frac{d\ln V}{d\ln R} - 1 = \frac{d\ln J}{d\ln R} - 2 = \frac{d\ln T}{2d\ln R} - 1 = \frac{d\ln M}{2d\ln R} - 3/2 \qquad \text{(A4)}$$

II NON AXISYMMETRIC FRAMEWORK

a) ellipticity ε of the ellipsoid of the stellar velocity dispersion in the approximation of negligible tangential forces (see e.g. Freeman, 1975). $\varepsilon = (V_R - V_\theta)/V_R$. V_R and V_θ are the radial and tangential components of the circular velocity

$$\varepsilon = \eta \qquad \text{(A5)}$$

b) frequency of kinematical bisymmetric disturbances $\Omega - \varkappa/2$; $\Omega + \varkappa/2$

$$\Omega - \varkappa/2 = \tilde{V}/R \qquad \Omega + \varkappa/2 = (2V - \tilde{V})/R \qquad \text{(A6)}$$

c) winding parameter $w = V_R/(\varkappa R)$ comparing epicyclic motions with the radial one (see e.g. Bertin, 1980):

$$w = (V_R/2V)\,(1-\eta)^{-1} \qquad \text{(A7)}$$

d) locations of the resonances. From the definition of corotation, inner Lindblad resonance and outer Lindblad resonance and by using (4) and the constancy of $\tilde{V}$ we get:

$$R_i = \frac{\tilde{V}}{V_o + V_1 R_c/R_{25}} R_c$$

(A8)

$$R_o = (2V_o - \tilde{V})/(V_o - V_1 R_c/R_{25})\, R_c$$

We want to stress that in most of applications we can

consider η as fairly independent of radius within a good approximation and then substitute it in (A1)-(A8) with its radially averaged value or its mean value $\langle\eta\rangle = \tilde{V}/V(\langle R\rangle)$.

Then, for each galaxy we can obtain the individual behaviour of density and angular momentum:

$$\rho(R) = \rho_{25} \, (R/R_{25})^{-2+s} \qquad \text{(A10)}$$

with $s = 4\,(1-\eta)^2 - 2$ and:

$$J = J_{25} \, (R/R_{25})^{1+p} \qquad \text{(A11)}$$

with $J_{25} = V_{25}R_{25}$ and $p = 1 - 4\,\eta + 2\,\eta^2$.

Since galaxies differ mainly in the value of $\tilde{V}$ rather than in the value of circular velocity, then we realize that **the mass distribution of dark matter is linked to the stellar disk angular momentum distribution.**

APPENDIX B

This appendix is aimed at pointing out that $\tilde{V}$ is strongly connected with many empirical aspects relevant to spiral structure. It is well known that, as general tendency, galaxies with rising rotation curves show a messy and filamentary arm structure, whereas galaxies with flat rotation curves show a global pattern (Whitmore, 1984). By means of the quantity $\tilde{V}$ we are able to quantify further this observational evidence:

1) We find a correlation between $\tilde{V}$ and the quantity GL introduced by Whitmore (1984) to describe the appearance of the spiral structure.GL ranges from 10 (poor spiral structure) to 30 (prominent spiral structure).In fact, "the degree of globality" of the spiral structure is found to increase accordingly to the value of $\tilde{V}$: from table 11 we can see that well-developed patterns are found in galaxies with high values of $\tilde{V}$ (and from (I.13) large sizes), whereas messy spiral structures are found in galaxies with low values of $\tilde{V}$ (and small sizes).

2) We found that none of 10 galaxies of sample A having $\eta < 1/5$ has a prominent spiral structure. Although we need a larger sample to make a more decisive statement, this limiting value might indicate the inability of a spiral galaxy to develop a global design if the steepness of its rotation curve exceeds a certain level $\left\{\frac{d\ln V}{d\ln R}\right\}_{R_{25}} > 0.28$.

GL	$\langle\tilde{V}\rangle$	N
10	26±6	5
20	43±5	18
30	60±4	13

TABLE 3

Averaged values of $\tilde{V}$ and their 1 σ scatter for the N galaxies belonging to sample A and having the same appearence of their spiral structure (same value of the index GL)

APPENDIX C

This Appendix is aimed to show that a linear fit to the observed rotation curves not only is very reasonable given the form of their profiles, but also necessary in order to prevent that non-circular motions strongly affect the determination of the large scale gradient of the circular velocity.

In order to infer the circular velocity from the observed rotational velocity, several method have been developed since the sixties; most of them are involved with the following prejudices:
1) rotation curves have a Keplerian fall-off ,$V(R) \propto R^{-1/2}$, at large galactocentrinc radii. (V is the circular velocity)
2) The greater the number of of parameters of the fitting functions, the more information we "extract" from the observations.

We shall show the 1) and 2) are so closely connected that the realization of the flatness of rotation curves puts high polynomial fits out.

In order to give an illustrative example we assume that the non-circular motions are due to the spiral gravitational potential which superposes a sinuisoidal perturbation ($\sim$ 10 %) on the axisymmetric one.

Then,

$$V_{rot} = V_o \, (R/R_o)^f (1 + \varepsilon \sin (R/\lambda)) \qquad (C1)$$

where f describe the large scale behaviour of the circular velocity; ε is the fractional amplitude of the spiral perturbation and λ is the radial length. A simple inspection of rotation curves gives:

$$R_{25}/\lambda = n \sim 3\text{-}5, \; \varepsilon \sim 0.1 \; , \; f = 0\text{-}0.3 \qquad (C2)$$

Then, by means of a high polynomial fit

$$V_{FIT} = \sum V_k R^k \qquad (C3)$$

with $k \gg 1$, we recover V_{rot} by fitting V_{obs} with (C3).

Let $|\Delta V/V|$ be the observational error , typically $\sim 10^{-2}$ and $|R/V\ \Delta(dV/dR)|$ the propagated error in the gradient of the rotational velocities. Then, from (2) we have:($\tau = R/R_{25}$)

$$|R/V\ \Delta(dV/dR)| = |\Delta V/V|\ \left|\frac{f(f-1)[1+\varepsilon \sin n\tau]+2n\tau f \cos n\tau - n^2\tau^2 \sin n\tau}{f[1+\varepsilon \sin n\tau]+n\tau\varepsilon \cos n\tau} - f + \frac{n\tau\varepsilon \cos n\tau}{1+\varepsilon \sin n\tau}\right| \qquad (C4)$$

atop the maxima $n\tau = \pi/2$, so:

$$|R/V\ \Delta(dV/dR)|_{max} = |dV/V|\ \left|\frac{f(f-1)(1+\varepsilon)-n^2\tau}{f(1+\varepsilon)} - f\right| \qquad (C5)$$

then, $|R/V\ \Delta(dV/dR)|_{max} \simeq n^2\ f^{-1}\ |\Delta V/V| \sim 1$ with typical values for n and f.

Thus, though high polynomial fits can draw V_{rot} very well, nevertheless they are not able to give the gradient of the circular velocity, being dV_{rot}/dR strongly affected by observational error. This is because both rotation curves are flat and the perturbative velocity field has a short scale oscillating behaviour. It must be said that if we assume a Keplerian fall-off for the circular rotation curve, $f \simeq 0.5$, this effect would not so serious.

We note that the crucial term in (3) would not be in a linear fit, being proportional to d^2V_{FIT}, which on the other hand, does not account for the perturbative component in the rotational velocity.

Therefore, we use the following procedure:

1) We assume:

$$V_{obs}(R) = V(R) + V_p(R) \qquad (C6)$$

with $V_p \ll V$ and $V_p(R)$ at least roughly periodical.

2) We linearly fit V_{obs}. Then, we see from 1) that perturbative velocity does not affect the coefficients of the fits V_o, V_1.

3) The perturbative velocity can be then obtained:

$$V_p(R) = V_{obs}(R) - V_o - V_1 R/R_{25} \qquad (C7)$$

In figure 5, V_p is plotted, we see that our assumption is confirmed: V_p does not show any large scale feature, being usually the imprint of a spiral gravitational perturbative potential.

FIGURE 5

Non-circular velocity component for some representative galaxies. The radial behaviour of V_p shown is the typical of all galaxies belonging to any our sample.

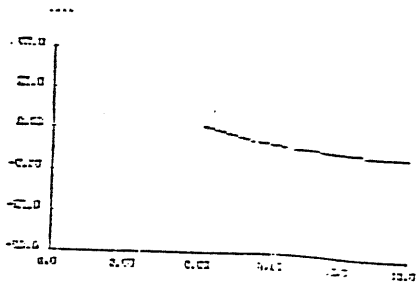

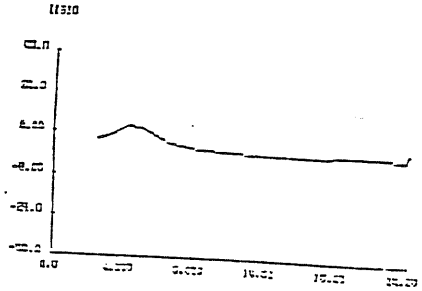

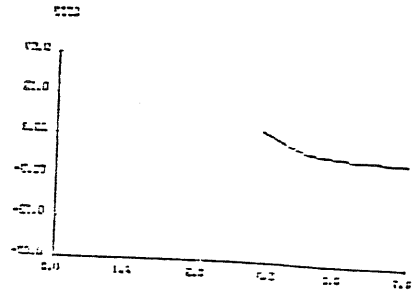

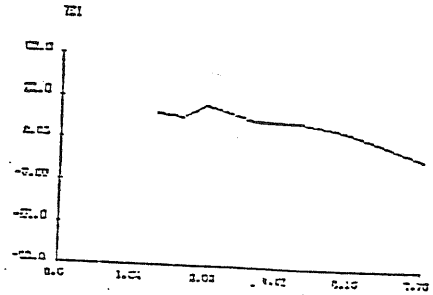

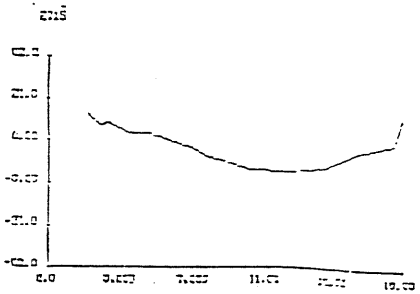

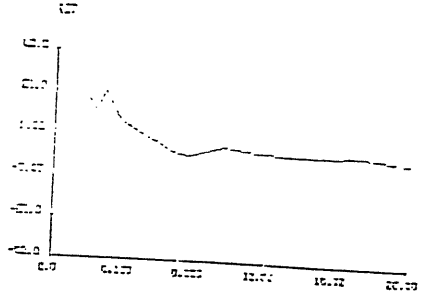

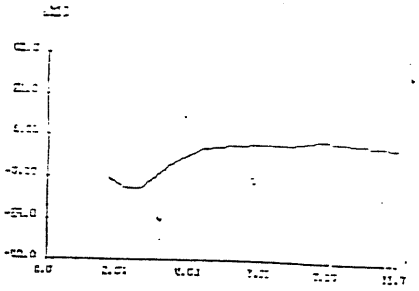

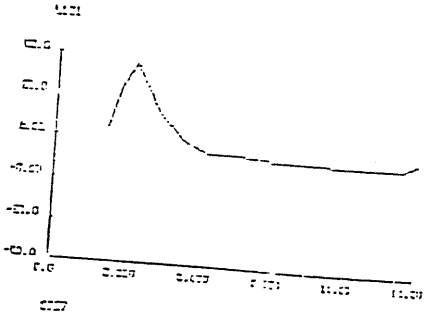

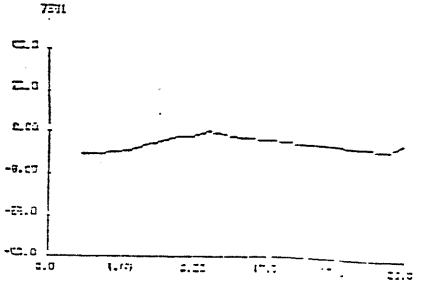

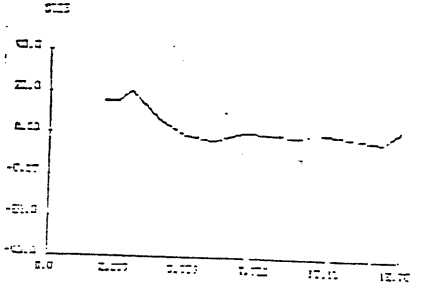

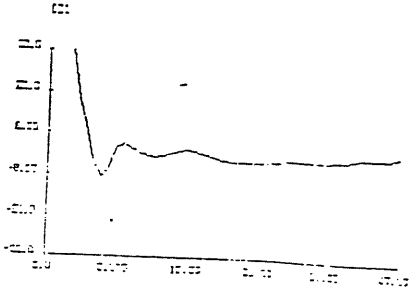

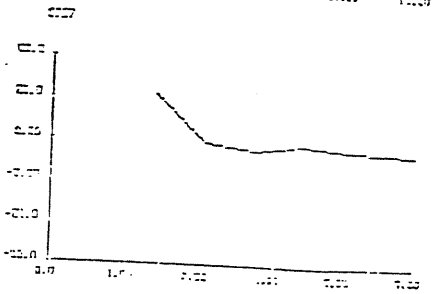

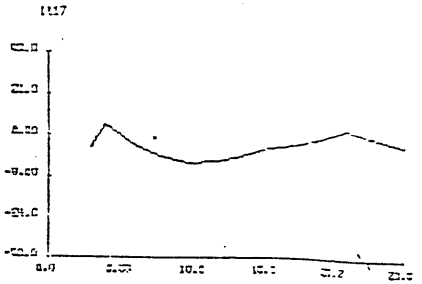

01

CHAPTER 2

GALAXY KINEMATICS AND GRAVITATION

I INTRODUCTION

Theoretical rotation curves for spiral galaxies, obtained by considering the luminous (baryonic) matter distribution strongly disagree with the observational ones which show non-decreasing, and even increasing gradients of circular velocity in the range 10-100 kpc. Then, by comparing dynamical densities (and total masses) with visible densities (and disk masses), two relevant questions immediately arise:

1) What is the "nature" of the matter detected only gravitationally ?

2) Why are visible and dark matter so strongly coupled ? This coupling often referred to as "fine" tuning of parameters of the visible and dark density distributions' can also be usefully seen in a model-independent way: the gradient of the circular velocity turns out to be completely dominated by the dark matter (see figure 6), nevertheless it correlates with disk properties (luminosity and size) better than typical disk velocities (Chapter 1 , Persic and Salucci, 1986).

Several explanations have been proposed to account for 1) and 2) , the most popular being the presence of non-baryonic cold dark matter (axions, photinoes, gravitinoes) clustering on galactic scales and surrounding the luminous disk. In this scenario question 2) is currently under investigation: the coupling is understood as a feedback effect on the dark halo by the dissipative infall of baryonic matter in its potential well (Blumenthal et al., 1986).

An alternative approach to answering 1) and 2) is to construct rotation curves using only the observed matter distribution but modifying Newtonian gravity law on galactic length scales in order to reproduce dynamical densities. Such a

modification is hoped to be the phenomenological manifestation on galactic sizes (and in the non-relativistic regime) of some (new) physical process in which gravitation is involved as partner of elementary particles fields (i.e. in strings, supergravity, and quantum gravity theories).

Nevertheless one thing should be made clear: any modification of gravitation law is (has to be), by far, more testable than a modification, within the framework of Newtonian gravity, of the theoretical scenario. So any gravitation theory which accounts for the rotation curve profiles with only the visible matter, must **automatically** answer question 2) and "predict" the relations found among galactic properties in the first Chapter.

The aim of this Chapter is to give a method of testing a **proposed** explanation of the "flatness" of rotation curves via a modification of gravity law, in order to show the absolute need for a deep preventive investigation of the whole observational scenario .

II THE FLAG MODIFICATION OF NEWTONIAN GRAVITY

One modification of the Newtonian law could arise naturally in the context of unified field theories which include gravity. Indeed, when attempting to include gravity in GUTS , due to the larger unification symmetry group, an additional massive gauge boson can exist (Sherk, 1979), giving rise to an extra matter coupling with a potential of the Yukawa form (for example in supergravity theories where the additional gauge boson acquire its mass via the super-Higgs mechanism, i.e. spontaneous breaking of supersymmetry).

Appealing to this highly symmetric description of nature Sanders (1984, 1986) has investigated a gravitation law containing a repulsive Yukawa component characterized by a coupling constant

α and a length scale R_o. Then for a point mass M the potential is:

$$\phi(R) = \frac{G_\infty M}{R}\left(1 + \alpha\, e^{-R/R_o}\right) \qquad \text{(II.1)}$$

where G_∞ is the gravitational constant measured at infinity and is related to the local value G_o by $G_o = G_\infty(1 + \alpha)$. Using the galaxy NGC 3198 as a calibration, the parameters α , R_o are fixed at $\alpha = -0.92\pm0.01$, $R_o = (36 \pm 4)(H_o/50)$ kpc to give a good fit to that rotation curve (using only the visible matter distribution). Then we see that the extra component of gravity is indeed repulsive and this modified gravity law is referred to as finite-length-scale anti-gravity (FLAG). Sanders then applied this FLAG potential to five others spiral galaxies ranging in size from 5 kpc to 40 kpc and produced flat rotation curves from a exponential thin disk density surface with reasonable $(M / L)_{disk}$ values.

III THE OBSERVATIONAL SCENARIO

Although the flatness of the circular velocity is a remarkable feature of a quite large fraction of spiral galaxies on the other hand we have that most of them show a **constant positive** gradient. (Rubin et. al. 1980, 1982, 1985; table 4, figure 5).

This observational evidence cannot be neglected, in fact a lot of information on individual differences of large scale properties is "stored" there: galaxies with steeper rotation curves have lower values of the circular velocity, are smaller and fainter too (first Chapter). In particular, how can be seen from table 4, the maximum circular velocity (or equivalently $V(R_{25}) \equiv V_{25}$, with R_{25} the 25 mag arsec^{-2} contour) is found to be strongly correlated with its gradient.

Again, an useful way to quantify this galaxy properties to investigate it by means of the quantity $\tilde{V}$. It is important to

recall its model-independent properties found in the first chapter:

1) $\tilde{V}$ is constant over the whole disk.

2) $\tilde{V} = F(V_{25}, (dV/dR)_{25})$ with $\partial F/\partial V_{25} \ll \partial F/\partial (dV/dR)_{25}$.

3) $\tilde{V}$ is a distance-independent quantity found able to correlate strongly with large-scale properties, such as radii and magnitudes and with local ones such as effective densities.

Thus, for sample B (let us recall that this sample contains all Sb-Sc non-local galaxies found in the literature with available rotation curve profiles) we have :

$$\log \tilde{V} = -(2.6 \pm 0.4) + (1.8 \pm 0.1) \log V_{25} \qquad \text{(II.2)}$$

This tight relation brings forth one condition for the effective potential ϕ of galaxies of very different masses and sizes (recall that $V^2 = R\, d\phi/dR$) :

$$7.4\ 10^{-2}(R_{25}(d\phi/dR)_{25})^{3/5} + 1/2\ (3 + (R\ d^2\phi/dR\ /\ d\phi/dR)_{25})^{1/2} = 1 \qquad \text{(II.3)}$$

It is important to stress that in the scenario involving a stellar disk embedded in a dark halo, relation (II.2),or equivalently (II.3), is an additional proof of the strong coupling between dark and visible matter. In fact, since approximately $R_{25}(d\phi/dR)_{25} \propto (M_b + M_{dark})$ and $(R\ d^2\phi/dR)_{25} \propto ((\rho_b + \rho_{dark})\ R^3 - 8\pi(M_b + M_{dark}))_{25}$, baryonic and dark masses inside and densities at R_{25} ,"cooperate", in order to realize relation (II.3).

On the contrary, in the FLAG scenario, due to the fact that only the visible matter is claimed to account for the observed kinematics ,we have that the modified ϕ_{FLAG} must satisfy (II.3) as its intrinsic property. Therefore, according to Sanders we have:

$$V_{25}^{FLAG} = G\ M_{disk} / R_{25}\ [1 + \alpha\ (1+R_{25}) e^{R_{25}/R_0}\ ]$$

(II.4)

$$\tilde{V}^{FLAG} = V_{25}\left\{1 - 1/\sqrt{2}\left[1 - \frac{1 + \alpha(1 + R_{25}/R_o + (R_{25}/R_o)^2)e^{-R_{25}/R_o}}{1 + \alpha(1+R_{25}/R_o)e^{-R_{25}/R_o}}\right]^{1/2}\right\}$$

Then we propose to test the FLAG scenario by investigating if (II.4) agrees with the observational property $\tilde{V} \propto V_{25}^{n}$ with $n = 1.8 \pm 0.1$.

We think that, independently of any theoretical criticism that can be raised against a modification of Newtonian gravity (the FLAG has been critically reviewed from a theoretical point of view by Sanders, 1986), it is important to observationally test gravity on a galactic scale.

More specifically we ask: within the FLAG framework does a sample of galaxies homogeneous to sample B satisfy (II.3) ?

IV THE TEST

To perform the test we randomly generated 50 Sb and 50 Sc galaxies with the same absolute blue magnitude M_B probability distribution of sample B. (Table 5)

For each galaxy R_{25} is found from the relations (Rubin et al. 1980, 1982, 1985):

Sb $$\log R_{25} = -4.2 - 0.26\ M_B$$

(II.5)

Sc $$\log R_{25} = -3.6 - 0.23\ M_B$$

Then, from (II.4), using (II.5), we find the slope k of the log $(\tilde{V}/M)$ // log (V_{25}/M) relation:

$$\tilde{V}/M \propto (V_{25}/M)^{0.75\pm0.04} \qquad \text{(II.6)}$$

Then n is found to be (recall that $V_{25}^2 \propto M$): n = k + 2(1 - k) = 1.25 ±.03 . This slope turns out to be statistically inconsistent with the observed one (n = 1.8 ± 0.1). We can qualitatively arrive at this conclusion too, simply by noting that according to the assumed potential, the smaller galaxies have a smaller logarithmic gradient than the larger ones: this is the exactly the contrary of the observations (Rubin 1980, 1982, 1986).

Then we can state that, although the assumed potential, that is a point mass with an additional Yukawa-like coupling is able to reproduce some feature of rotation curves, nevertheless it is unable to account for the more detailed properties of the total effective potential we observe in spirals.

V CONCLUSION

The (rough) constancy of rotation curves is only one of many properties of the effective axi-symmetric potential we have to deal with. In an orthodox framework such properties describe phenomenologically the present structure of spirals and the late stages of their formation; instead, in a non-orthodox scenario involving modifications of Newtonian law, this properties must "trivially" and naturally turn out.

In particular, we applied this strategy to the Sanders modification of Newtonian law: we find that the assumed potential is insufficient to account for the relevant observational evidence that smaller galaxies have steeper rotation curves. However, it

important to note that the test performed here involves the potential assumed, not the underlying scenario. More generally, We suggest that alternatives to dark matter take the whole observational scenario very seriously, We feel in fact that such a strategy is able to spectacularly prove one of them or straightforwardly show their irrelevance.

V	N	$\langle \nabla \rangle_{25}$	σ
100-150	12	0.37	0.07
150-200	14	0.28	0.06
200-250	20	0.16	0.06
250-300	13	0.14	0.05

TABLE 3

Mean values of the logarithmic gradients at R_{25} for galaxies whose maximum circular velocity is in a range indicated in the first column. N is the number of galaxies of sample B found in each range and σ is the 1-σ scatter.

M_B	p
19-20	0.07
20-21	0.22
21-22	0.32
22-23	0.34
23-24	0.05

TABLE 5

Probability p of detecting a galaxy of sample B in the magnitude range indicated by the first column.

CHAPTER 3

HALO AND DISK INTEGRAL PROPERTIES

I INTRODUCTION

The shape of rotation curves is a strong indicator for the presence of non-luminous matter even in the limit of optical disk. (Faber and Gallagher, 1979; Rubin et al., 1980; 1982; 1985; Carignan and Freeman, 1985; Chincarini and de Sousa, 1985). Nevertheless, despite this overwhelming evidence, the visible/dark matter decomposition in each galaxy is still uncertain and controversial (Burstein and Rubin, 1983; 1986; Carignan and Freeman, 1985; Bahcall and Casertano, 1985; Kent, 1986; van Albada and Sancisi, 1986). In fact, even integral properties, as the amount of dark matter inside the optical radius, turn out to be very dependent on assumption made and on mass model used, so that a systematic study of the (derived) halo and disk properties seems to be unreliable.

The difficulties in studying the late stages of galaxy formation arise precisely from this lack of knowledge on fundamental galaxy properties. In fact, the formation of the diskinvolves a dynamical coupling between the dissipative and the collisionless components; this coupling leads to the present local and integral properties through a process whose (important) details depend both on the initial dynamical state of the proto-haloes and on the "astrophysics" of the infall. Thus, the spectrum of cosmological perturbations, the properties of proto-haloes, the infall of baryonic matter and the present structure of galaxies are so connected each other that cannot be treated separately.

The aim of this work is then to derive halo and disk

properties in order to systematically study them in the light of galaxy formation theories. Here the decisive improvement, which enable us to obtain them, comes from the realization that many of the individual basic properties of spirals are "imprinted" on the profiles of rotation curves (i.e. on their gradients). Thus, we can successfully use this observational evidence in order to overcome the difficulties present in any baryonic/dark matter decomposition which basically originate from the fact that we do not know: a) how to exactly link the luminosity of the disk with its mass b) how the dark matter is distributed inside the optical radius.

The plane of this work is the following: in section III we show the basic formalism developed to obtain disk/halo mass ratios; the (simple and reasonable) assumptions made are previously discussed and checked in section II. In section IV the (derived)disk properties are investigated: then a theoretical justification for the Tully-Fisher relation is worked out; moreover we are able to improve it by taking into account systematic differences of the fraction of dark matter present along the luminosity sequence. In section V we discuss our results in the light of different dark/visible mass decomposition strategies. In section VI we investigate the halo properties under the assumption $M_{lum}/M_{tot} = 0.1$: the derived halo densities and sizes provide us with the (auto)correlation function $\xi(R)$.

The sample of galaxies (hereafter sample C) we have used for systematic investigation comprises all the (43) non-local Sa-Sc galaxies for which both high-quality extended rotation curve and good photometry are available (Data are in table 6) Local galaxies are left out because their distances, and therefore any distance-dependent quantity, are quite uncertain. Of course this problem still remains, although probably reduced, also for galaxies whose distance is derived from the redshift, nevertheless this choice avoids the mixing of galaxies with distances obtained from local calibrators with those with distances obtained from redshifts.

II SPIRALS : PHOTOMETRY, ROTATION CURVES AND DARK MATTER

In this section we address the direct observational properties of spiral galaxies and the implications on structure models. Since the detection of a (large) fraction of total matter only by means of its gravitational interaction is a recurring feature for spiral galaxies, then we fix on general properties and neglect any occasional or clearly unrelated characteristic.

a) The distribution of light.

Most of the galaxies are decomposed in two main luminous components (Freeman, 1970; Boroson 1981; Kent, 1984; 1986; van der Kruit 1986; Simien and de Vaucouleurs 1986): a very concentrated bulge and a thin disk with exponential decrease of surface density I(R):

$$I(R) = I_o e^{-R/R_D} \qquad \text{(III.1)}$$

with R_D the exponential length scale. The bulge is usually less luminous and more concentrated than the disk (Simien and de Vaucouleurs, 1986) : L_B / L_D = .7 for Sa and .1 for Sc ; R_{25}/R_B = 8-16, where R_B is the effective bulge radius, and R_{25} is the 25 mag arsec^{-2} contour ; then bulge contribution to equilibrium structure is usually negligible for $R \geq 2 R_B$. This is definitively proved by the fact that the profiles of rotation curves are found uncorrelated with the bulge/disk ratio (Rubin et al. 1986). Since, in agreement with a constant mass/light ratio, disk colors do not show any substantial gradient, then we can safely assume:

$$R\ (d\phi/dR)_{lum} \cong R\ (d\phi/dR)_{disk} \equiv V_D^2(R) \qquad \text{(III.2)}$$

where ϕ_{lum} is the gravitational potential of all the luminous

matter and V_D^2 is the circular velocity for the exponential thin disk model.

b) Rotation curves.
In the literature ~ 100 extended (out to R_{25}) optical rotation curves are available: practically no show any large-scale variation of its gradient (being in same case strictly zero). So:

$$V(R) = V_o + V_1 (R/R_{25}) \qquad \text{(III.3)}$$

for $R \geq R_B$, where $R_B \simeq$ 0.1-0.2 R_{25} is the radius from which onward V(R) takes a linear behavior.

A phenomenological model-independent investigation of properties of the circular velocity field along the luminosity sequence has been carried out in Persic and Salucci (1986) (see also Chapter I). The results are:
1) The total increase of the circular velocity outside the bulge region is not negligible (in fact the observed $\left|\frac{d\log V}{d\log R}\right|_{25}$ of the supposed "flat" rotation curves, in average, turns out to be as large as the expected $\left|\frac{d\log V}{d\log R}\right|_{25}$ for the falling rotation curves of the exponential thin disk model), moreover it is found to be correlated to the integral properties better than a typical reference velocity.
2) Spiral galaxies form, with respect to their integral properties, a one-parameter sequence. A useful way to realize it is to introduce the quantity $\tilde{V} \equiv (\Omega - \varkappa/2)$ with $\varkappa^2 = R\, d/dr\, (V^2 R^2)$, then, as shown in the previous Chapter: $M_B \propto \tilde{V}^2$, $M_H \propto \tilde{V}^2$, $V_{25} \propto \tilde{V}^{1/2}$, $M_{HI} \propto \tilde{V}^2$, $R_{25} \propto \tilde{V}$, where M_B and M_H are, respectively, the blue and infrared magnitude and M_{HY} is the neutral hydrogen mass. So, smaller galaxies (and fainter too) have a larger gradient of the circular velocity. It is important to stress that these latter relations are by far weaker if we use as a parameter any velocity-controlled quantity.

This phenomenological, but model-independent, investigation strongly indicates 1) dark matter and visible matter are coupled

2) dark matter has different dynamical importance along the luminosity sequence. In fact, this is the only case in which the **luminosity/kinematics relation can become tighter by correlating the gradient of the circular velocity instead of the maximum velocity.**

c) Dark matter

The discrepancy between the visible matter and the total matter inferred from the rotation curve comes out immediately from the profiles of the rotation curves. To this purpose it is worthwhile to compare the dynamical $(\frac{\tilde{V}}{V})_{dyn} = \frac{\tilde{V}}{V_o + V_1 (R/R_{25})}$ with the luminous one:

$$\left(\frac{\tilde{V}}{V} \right)_{lum} = 1 - \left(\frac{I_o K_o + 1/2\ R/R_D (I_1 K_o - I_o K_1)}{2\ (I_o K_o - I_1 K_1)} + 1/2 \right)^{1/2} \qquad \text{(III.4)}$$

where I_o, K_o, I_1, K_1 are the modified Bessel functions evaluated at $(1/2\ R/R_D)$.

The clear advantage of this method, with respect to that of comparing $V^2_{dyn}(R)$ with $V^2_{lum}(R)$, is that $(V/V)_{lum}$ does not depend on $(M/L)_D$, so both $(\tilde{V}/V)_{lum}$ and $(\tilde{V}/V)_{dyn}$ are directly measured. Then, we immediately realize that a dark component is needed along the disk in order to keep constant dV_{obs}/dR .

The discrepancy between $(\tilde{V}/V)_{lum}$ and $(\tilde{V}/V)_{dyn}$ cannot be eliminated or reduced by a possible bulge or stellar halo contribution.

In fact, since $\rho_* \propto r^{-3}$ or $\rho_* \propto r^{-7/8} \exp(-r/r_o)$ (Bahcall et al., 1983) and the bulge is a point mass for $R \gg R_B$, then $(\tilde{V}/V)_{halo}$ and $(V/\tilde{V})_{bulge}$ are even steeper than $(\tilde{V}/V)_{disk}$, so that their inclusion in $(\tilde{V}/V)_{lum}$ increases the discrepancy. On the contrary if we compare $\tilde{V}_{lum}$ with $\tilde{V}_{dyn}$ the present discrepancy can be reduced by adding a bulge or a stellar halo contribution with suitable (M/L)'s.

Figures 5a-5g , independently of and in addition to the 21 cm rotation curves showing a constant circular velocity out to 10 disk length scales (Bosma, 1981; van Albada, 1985; van Albada and Sancisi, 1986), calls for some amount of dark matter within the optical disk.

It is very unlikely that it resides in the disk, let us consider the two cases: non-baryonic and baryonic dark matter. In the first case it is almost impossible to confine collisionless matter in a disk-like configuration, in the second case is difficult to understand why a possible dissipative baryonic dark matter is distributed in the disk so differently from the visible one; moreover, serious problems arise when baryonic candidates (snowball, dust, rocks, planets, stars, dead stellar remnants) are considered (Hegyi and Olive, 1983, 1986).

In addition, there are some observational arguments against a disk-shaped dark matter distribution and in favor of a spherical one:

1)in three polar ring S0 galaxies the comparison of velocities in the disk with those in the ring, strongly supports a nearly spherical distribution of dark matter (Whitmore et al., 1986; Schweizer et al., 1983)

2)By means of the ratio between the z to the radial component of the Galactic acceleration field we are able to discriminate the shape of the dark matter distribution. Although this topic is still debated (Oort missing mass) we can safely state that, at the sun, the amount of dark matter needed to have a flat rotation curve cannot reside in the disk (Rohlfs, 1982).

Therefore, throughout the paper we assume a dark matter halo surrounding an exponential thin disk.

A good approximation of contribution of dark matter to the circular velocity at the optical radius can be evaluated without assuming any specific halo mass distribution: let us define $\gamma \equiv V_D^2/V_H^2$ (H refers to dark halo and all quantities are evaluated at

R_{25}) Then, we have:

$$(2\,(\tilde{V}/V_{25} - 1)^2 - 1)_{obs} = (2\,(\tilde{V}/V_{25} - 1)^2 - 1)_D\ \gamma/(1+\gamma) + (2\,(\tilde{V}/V_{25} - 1)^2 - 1)_H/(1+\gamma) \qquad \text{(III.5)}$$

The condition $dV/dR \geq 0$ requires:

$$(\tilde{V}/V)_H \leq \langle (\tilde{V}/V) \rangle \leq (\tilde{V}/V)_D \qquad \text{(III.6)}$$

Then, provided that $0.2 \leq \gamma \leq 5$, we have:

$$\gamma \simeq \frac{1 - (\tilde{V}/V - 1)^2}{(1 - \tilde{V}/V)^2 - (1 - \tilde{V}/V)_D^2} \qquad \text{(III.7)}$$

The values for individual galaxies are reported in table 7 : we want to stress that we cannot consider γ even fairly constant along the luminosity sequence of galaxies, approximately: $\gamma \propto L_B^2$. A very important consequence of (II.7) is that we can understand the physical grounds of Tully-Fisher (1977) relations (hereafter TF): in fact from the condition of centrifugal equilibrium (at R_{25}) we have:

$$M_d \propto V_{25}^2 (1 + 1/\gamma)\ R_{25} K(R_{25}/R_D) \qquad \text{(III.8)}$$

with $K(x) = 1/2\ x^3 (I_0 K_0 - I_1 K_1)$, and the modified Bessel functions are evaluated at $1/2\ x$, note that, for $x \geq 3$ $K(x) \simeq 1.34$.

The central surface brightness I(0) is peaked around the value 21.65, (Freeman, 1970; Boroson, 1981; van der Kruit, 1986;) this implies both a small scatter in the values of R_{25}/R_D and the relation $L_B \propto R_{25}^2$. So, in the case γ = constant, from (III.8) we

recover the usual TF relation $L_B \propto V_{25}^4$. Moreover from (III.8), we predict that part of the scatter is intrinsic arising from the different percentage of dark matter along the luminosity sequence.

This effect, however, can be taken into account by using (III.7), therefore we correlate L_B with M_D, being both two different "measures" of the disk luminosity. We find:

$$L_B/L_\odot = .72\ (M/M_\odot)^{0.78\pm0.07} \qquad \text{(III.9)}$$

$$r = 0.85 \qquad \sigma = 0.55 \text{ mag}$$

Then, TF relation is the γ = const. limit (same fraction of dark matter in all galaxies) of the centrifugal balance of a rotating self-gravitating disk embedded in a spherical halo. Nevertheless, the fraction of dark matter is correlated with the total luminosity ($\gamma \propto L_B^2$), this implies a reasonably small scatter also for the TF relation and allows us to take into account its differences along the luminosity sequence. Consequently we are able to reduce the scatter by $\sim$ 0.2 mag.

Above we have investigated, in a model-independent analysis, global properties of the visible matter and the importance of dark matter in the structure equilibrium. A further important point is: how dark matter is distributed ? To this question we can answer directly (Fall and Efstathiou, 1980), in fact we have:

$$\rho_H = S(R) - S_D(R) \qquad \text{(III.10)}$$

with :

$$S(R) = \frac{1.2\ 10^{-27}}{R^2}\ (V_o + V_1\ R/R_{25})\ (V_o + 3\ V_1\ R/R_{25})$$

$$S_D(R) = 3.4\ 10^{-26}\ (M/L)_D\ L_o/R_D\ (1.5\ I_oK_o - .5\ I_1K_1 - .5\ R/R_D\ (I_oK_1 - I_1K_o))$$

In (III.10) we use the (M/L)'s obtained from the B-V by means of Larson-Tinsley (hereafter LT) evolutionary models (Tinsley, 1981)

In all galaxies, for a large range of values of $(M/L)_D$ around the LT one, we find:

$$\rho(R) \simeq \frac{\rho_o}{1 + (R/a)^2} \quad , \quad R_{25}/a \approx 1 \qquad \text{(III.11)}$$

In detail, for each galaxy we analyzed 5 different solutions of (III.10) having different values of the parameter $(M/L)_D$; firstwhole, we compare the value derived from LT with this of the maximum disk hypothesis (van Albada et al. 1985, Carignan and Freeman, 1985, van Albada and Sancisi, 1986) (that is by maximizing the disk contribution to the structure model in the inner part of the galaxy: $S_D(R) = S(R)$); if it is lesser we take: $0.75 \leq (M/L_B)/(M/L_B)_{LT} \leq 1.25$, otherwise: $0.5 \leq (M/L_B)/(M/L_B)_{MAX} \leq 0.9$.

We found ,practically in all cases, that (III.11) describes to high accuracy (level of significativity > 6 σ), in a large outer part of a galaxy the dark matter density distribution. Just in a few cases, near to the maximum disk solution, we found $\rho(R) \approx$ constant. Moreover we are able to constrain the core radius, we find $R_{dn}/a \simeq 1 \pm 0.5$.

It is important to stress that, despite its 'exact' formulation, (III.10) cannot be considered useful as first step in the derivation of global properties of galaxies, in that any integral property obtained by this method is very dependent both on the (unknown) value of $(M/L)_D$ and on possible errors on the determination of the distance of the galaxy.Then, let's notice that we used it just in order to show that, independently of any reasonable value of S_D/S , at any point within the disk, the pseudo-isothermal density law describes satisfactory the mass distribution of dark matter.

III THE BASIC FORMALISM AND THE DISK/HALO MASS RATIO

In deriving halo and disk integral properties the basic idea is to minimize the effect of a poor knowledge of: 1) local quantities, such as the density of dark matter, 2) global quantities, such as bulge (stellar halo) mass and disk mass-to-light ratios. Thus, instead of starting off with local and/or unknown properties, construct theoretical rotation curves and therefore, by imposing that these match the observed rotation curves, derive the relevant integral quantities, we address directly this achievement. This is made possible after the realization that **individual differences among galaxies lie mainly in their profiles of rotation curves rather than in their distinct dark and visible matter distribution.**

Then, with a minimum of assumptions (moreover supported by the the results of the previous section) on visible and dark matter mass distribution we obtain disk and halo integral quantities directly from the rotation curves; of course local quantities still remain poorly unknown, so as any integral one which not significantly affects the **total** distribution of mass.

To this purpose, we compare (at R_{25}), by means of Poisson equation, the implied $(d^2\phi/d^2R)_{model}$ with the observed $d^2\phi/d^2R$. Let $\phi(R)$ the total effective gravitational potential in the plane of a galaxy:

$$d\phi/dR = V^2/R \qquad \text{(III.12)}$$

Then,

$$(d^2\phi/d^2R)_{obs} = \frac{V^2}{R^2}\,[4\,(1 - \tilde{V}/V)^2] \qquad \text{(III.13)}$$

Therefore, we assume a two-component mass model: 1) an exponential thin disk with surface density proportional to surface brightness density (II.1) and 2) a spherical halo with volume density $\rho(R)$:

$$\rho(R) = \frac{\rho_o}{1 + (R/a)^2} \qquad \text{(III.14)}$$

with a the core radius. In the previous section we have shown that this density law is strongly suggested by a systematic comparison of the total effective mass distribution with the visible one; Moreover, simulations in a flat cold dark matter Universe produce proto-haloes structures with density law similar to (III.14) (Frenk et al., 1985; Hoffman and Shaham, 1985; Quinn et al., 1986).

The condition of centrifugal equilibrium is:

$$V^2 R = G \left(M_{halo}(R) + K(R)\, M_{disk}(R) \right) \qquad \text{(III.15)}$$

then:

$$\left(d^2\phi/dR^2\right)_{obs} = G/R_{25}^2 \; d/dR \left(M_{halo}(R) + 1.34\, M_{disk}(R)\right)_{25} \qquad \text{(III.16)}$$

Thus, from (III.1) (III.13) (III.14) (III.16) with some manipulations we obtain the equation:

$$0.89\, e^{-x}\, \hat{\beta} + \frac{y^2}{(1 + y^2)(y - \text{arctg } y)}(1 - \hat{\beta}) = 4\, (1 - \tilde{V}/V_{25})^2 - 1 \qquad \text{(III.17)}$$

with $x = R_D/R_{25}$, $y = R_{25}/a$ and $\hat{\beta} = M_D/(G^{-1}\, V_{25}^2 R_{25})$.

The disk/halo mass ratio $\beta = M_D/M_H$ (with $M_H \equiv M_{halo}(R_H)$) is then:

$$\beta = \frac{\hat{\beta}}{1 - 1.34\,\hat{\beta}} \qquad \text{(III.18)}$$

From (II.17) (II.18), $\beta = \beta(\tilde{V}/V_{25},\ R_{25}/R_D,\ R_{25}/a)$, where $\tilde{V}/V_{25}$ and R_{25}/R_D are observable, while R_{25}/a is not. It is important to stress that, for the range of values of R_{25}/a found in the sample and in agreement with those from N-body simulations, β depends very weakly on R_{25}/a, its main dependence being on the "slope" of rotation curve $\tilde{V}/V_{25}$, (see figure 7. So, we can consider R_{25}/a fairly constant along the luminosity sequence and to work out its average value $\langle y \rangle$ by minimizing the scatter Σ of the M_B // V_{25}^2 β relation Of course for self-consistency we require:

$$\Sigma(\langle y \rangle) \leq \Sigma(TF) \qquad \text{(III.19)}$$

with $\Sigma(TF)$ the scatter of TF relation; for sample C, $\Sigma(TF) = 0.73$

Then, we minimize Σ under the constrain (III.19):

$$\partial\Sigma/\partial(\langle y \rangle) = 0 \qquad \text{(III.20)}$$

By solving (III.20), we find $\langle y \rangle = 0.75$; moreover (III.19) is fulfilled if

$$.5 \leq \langle y \rangle \leq 1. \qquad \text{(III.21)}$$

So the range in β induced by the allowed range in R_{25}/a is about five times smaller than those induced by the derived range in the velocity slope. Therefore, hereafter we assume y = 0.75

Then, we work out the values of β for the galaxies of sample C (Table 9) ; we realize that β is very sensitive to the distribution of total matter but it is much less sensitive to the

structure parameters of the single components. Thus, **the disk/halo mass ratios shape the rotation curves of galaxies by determining their slopes.** Figure (7) shows that β spans a wide range of values, being smaller in faint galaxies (lower values of $\tilde{V}/V_{25}$)and larger in the luminous ones. In fact, we find:

$$M_B = (-21.2 \pm 0.14) - (2.6 \pm 0.3) \log (M_d/M_H) \qquad \text{(II.22)}$$

$$r = 0.68 \qquad \sigma = 0.75$$

that is $M_D/M_H \propto L_B$.

This is the model-dependent counterpart of relation (II.7) and it explains why in spite of the presence of dark matter (different from galaxy to galaxy), the blue magnitude correlates with the maximum velocity (i.e. with the total matter inside the optical radius): in fact, the amount of visible matter, responsible for the luminosity, correlates to the amount of dark matter present within the optical disk. This is the imprint of a dynamical coupling between dark and baryonic matter during the infall of this latter in the proto-halos potential walls (e.g. the push in effect that the infalling baryonic matter has on the collisionless halo (Blumenthal el al. 1986; Flores et al., 1986). Although details of such a coupling have still to be investigated, its result is clear: **spiral galaxies form with respect to their mass distribution a one-parameter sequence.**

A further consequence of (III.22) is that, according to the scenario in which $M_{lum}/M_{tot} = 0.1$ on all scales and therefore the total halo mass is 10 times the disk mass, the halo of a faint, small disk does not extend much beyond its isophotal radius, while in the case of a brighter and larger galaxy the halo's size exceeds the disk's by a large factor

IV. THE DISKS: LUMINOSITIES, COLORS AND KINEMATICS

It seems appropriate to couple the light with the disk-related dynamics, so that both "measure" the same mass component. This is not clearly the case if the luminosity is coupled with some total reference velocity, M_D/M_H not being a constant quantity along the luminosity sequence. By means of arguments similar to those of section II we expect $L_B \propto V_D^4$ with $V_D = \sqrt{\hat{\beta}}\, V_{25}$ the disk rotation velocity at R_{25}. we find (see fig. 9):

$$M_B = (-9.8 \pm 1.1) - (5.4 \pm 0.5) \log V_D \qquad \text{(III.23)}$$
$$r = 0.80 \qquad \sigma = 0.61$$

that implies $L_B \propto M_D^{1.1\pm0.1}$. With respect to TF relation (III.23) has smaller scatter (about 0.1 mag) and is significantly flatter (see figure 8), for sample C the TF relation implies $L_B \propto M_D^{1.6\pm0.2}$, and nearer to the theoretical proportionality between luminosity and disk mass. Note that the correction for the presence of dark matter is more important for low-luminosity galaxies. Of course a constant M_D/M_H along the luminosity sequence would have yielded the same slope in TF relation and in (III.23).

Moreover, we can explain, in the light of relation (III.23), why $\tilde{V}$ is a better discriminant of luminosity and optical size than the maximum velocity. In fact from (III.17) and (III.18) we have that the model-independent quantity $\tilde{V}$ is statistically equivalent to the (model-dependent) disk velocity (in detail: $\tilde{V} \propto V_{25}^{1.1}$ r =

0.99), so that $\tilde{V}$ 'weighs' directly the disk mass, neglecting automatically the dark matter contribution in V_{25}.

The disk velocity is also found to be linearly correlated with the optical radius:

$$\log R_{25} = (-0.87\pm0.23) + (1.0\pm0.1) \log V_D \qquad (II.24)$$

with r = 0.82 .This implies the existence of a characteristic disk rotational frequency $\Omega_D = V_D/R_{25}$ common to all galaxies, regardless of their very different luminosities, sizes and morphological types. The value $\Omega_D = 7.4 \pm 1.1$ km s^{-1} kpc^{-1} is then a regularity that theories of disk formation and angular momentum acquisition should account for.

From β's it is possible to calculate the mass-to-light ratio of the disks. Theoretical studies based on stellar population synthesis definitely predict a correlation between colors and M_D/L_B ratios: from Tinsley (1981) for the case of a continuous star formation we deduce $\log M_D/L_B = - 0.8 - 1.85$ (B-V). For sample C we obtain (figure 11):

$$\log M_D/L_B = (-0.83\pm0.15) - (1.91\pm0.24) (B-V) \qquad (III.25)$$

with r = 0.68 .

V DISCUSSION

At this point it is worthwhile discussing our results in the

light both of other strategies of dark/visible mass decomposition and of different "measurements" of the visible to dark mass ratio.

Firstwhole, let us discuss the maximum disk hypothesis (MDH), that is the suggestion that in the inner regions of the galaxy (say at $R = 2\ R_D$) disk matter dominates the dynamics. Then, via an assumed halo density distribution, usually a pseudo-isothermal one with central density and core radius as free parameters, basic halo properties are worked out by fitting the differences between the observed rotation curve and the exponential thin disk one.

Nevertheless, despite its promising simplicity, we have several arguments indicating that such a hypothesis needs careful examination case by case and should be taken as a constraint on the maximum value allowed for the disk mass-to-light rather than a working procedure of dark/visible mass decomposition. In fact:

1) MDH, obviously, is strongly biased against finding remarkably large amounts of dark matter in the inner parts of galaxies and even within the optical size. Since a priori we have not any theoretical suggestion leading to that, this prejudice does not seem to be a suitable property for a dark/visible mass decomposition strategy. Moreover, we know some examples indicating large amounts of dark matter even within the optical sizes. (Whitmore et al., 1986 , Comte , 1986)

2) Let suppose that the dark mass is negligible in the innermost part of the galaxy. Unfortunately , in many cases, where the dark halo is negligible, there, the bulge is not. Of course, in theory, we could account for it by means of a bulge mass model

derived from the luminosity distribution (Kent, 1986), nevertheless this seems to bring unnecessary complications which arise only because we insist in comparing dynamical masses with visible masses in the inner regions rather than at the optical size. In fact some difficulties come out immediately when MDH is applied to a large sample of galaxies (Kent, 1986 ; 37 galaxies, sample C shares most of them)): for 2 galaxies Kent found non-physical solutions, in another 12 $(M/L)_D$ exceeds $(M/L)_B$, sometimes even by a factor 5. This is in strong contrast with the observational evidence of the systematic color gradient (reddening moving towards the nucleus) found in early type spiral galaxies (Visvanathan and Griesmith, 1977; Griesmith, 1980), that is in contrast with the well-known fact that bulges are ordinarily much older than disks.

3) Let us consider bulgeless systems, about 40 % of galaxies in sample C; In the previous section we have seen that the discrepancy between the observed profile of the rotation curve and that derived by the disk distribution of mass starts even in the very inner region of the galaxy (fig. 5).Then, for these galaxies is very hard to assume that the amount of halo matter at 2 R_D is negligible. It is important to stress that practically in every galaxy the rotation curve profile strongly deviates from that of an exponential thin disk even well before that the disk component would have given its maximum contribution.

4) Not unexpectedly the $(M/L_B)_D$ values implied from the MDH turn out systematically higher than the LT ones (Larson and Tinsley, 1978). From Kent, we have $\langle (M/L_B)_D \rangle_{MDH} \simeq 3.4$, while the corresponding average value from LT model is 1.9. This

discrepancy is also present in the MDH derivation of basic parameter of dark halo in four late-type spirals done by Carignan and Freeman, (1985) , in fact for NGC 247 there is a factor 2 between the two values, and for NGC 300 and NGC 3109 the consistency is found only accepting an enormous amount of gas mass.

5) When MDH has been applied to very small samples of galaxies it seemed that it yields a dark/visible mass ratio constant among galaxies (Carignan and Freeman, 1984; Bahcall and Casertano, 1985; van Albada and Sancisi, 1986) nevertheless after Kent (1986) the situation is more complicated. In fact the MDH solutions in his sample (37 objects), indicate that, at the optical radius, in $\sim$ 1/4 of cases the halo mass is negligible, in $\sim$ 1/4 of cases is predominant and half of galaxies lie between these two extremes.

We want to stress that both our methods for deriving integral halo and disk properties are not biased against the MDH at all. They are completely indifferent to this hypothesis so that they eventually would be able to prove it.

Let us remember that according to our results, MDH might be a working hypothesis in large and luminous galaxies, being in these galaxies the presence of an amount of dark matter necessary but relatively small. On the contrary, our results strongly contrast the MDH in faint galaxies found halo dominated. We think that in these galaxies MDH set only a constraint on the maximum disk mass that the dynamics allows.

There are independent evidences that support our picture:

1) Tinsley comparing dynamical (M/L)'s with those inferred from the LT models found that bluer galaxies have more massive dark halos(Tinsley, 1981). Then, the color-magnitude relation (Wyse, 1982; Tully et al., 1982) implies that the contribution of dark matter to the dynamics is larger in the more luminous galaxies (see also Vader, 1984).

2) Whitmore et al. measured directly the flattening of equipotential in three S0 polar ring galaxies at 0.6 $R_{25} \sim$ (2.5 - 3) R_D ; the main results they found is that in these galaxies, even in the relatively inner regions, a nearly spherical halo must be the dominant massive component. Moreover, if we infer the dark/visible mass ratio by means of the scale/free gravitational potential of Monet, Richstone and Schecter (1981), we agree even quantitatively with their results (Whitmore et al. , 1986) $\beta \sim 0.1$ for galaxies with $M_B \approx -20$.

3) There are evidences that faint galaxies are halo dominated also for the other tail of the Hubble sequence. Compte (1986) analyzed a sample ($\sim$ 10 galaxies) of local irregular and magellanic-like galaxies. The differences between the total observed total gravitational potentials and those due to a flat disk allow him to obtain the dark/visible mass ratios: he finds that practically all galaxies in his sample are halo dominated, $\beta \sim 0.1$ (de Vaucouleurs distances scales)

4) As well-known the infrared version of TF relation (Aaronson et al., 1982) shows interesting features a) the slope is steeper for low luminous galaxies and approaches only asymptotically the value of 10 b) faint galaxies lie

systematically below the curve obtained for high luminosity galaxies c) this effect increases monotonically towards low magnitudes.These features fit perfectly with our picture: in the previous sections we found that only very luminous galaxies have a quite negligible fraction of dark matter, so that the slope 10 is reached only for the brilliant tail of the luminosity sequence; therefore, since fainter galaxies have a larger contribution to the dynamical mass due to non luminous matter, then, they will result less luminous than we expected on basis of the behaviour of brilliant galaxies. Moreover, since the disk/halo mass ratio increases with the luminosity, this effect must increase when luminosity decreases.

VI. THE HALOS: DENSITIES AND SIZES

The internal densities of the halos averaged within the optical radii are found to be tightly coupled to the photometric sizes of the disks:

$$\log \langle \rho_H \rangle_{25} = (-22.1 \pm 0.2) - (1.86 \pm 0.20) \log R_{25} \qquad \text{(III.26)}$$

with r = 0.88 : density and sizes hereafter are measured in $g\ cm^{-3}$ and kpc, respectively. Assuming the popular view that $M_{lum}/M_{tot} = 0.1$ on all scales (Blumenthal et al. 1984), it is possible both to calculate the halo radius R_H and the mean halo density $\langle \rho_H \rangle$, provided that dark matter is still approximately distributed according to (III.14) at very large distances. Again a density/radius correlation is found (figure 12):

$$\log \langle \rho_H \rangle = (-22.1 \pm 0.2) - (1.77 \pm 0.15) \log R_H$$

(III.27)

with r = 0.91.

It is very important to realize that halos and disks sizes are linked, in fact we find:

$$R_H/R_{25} \simeq R_{25}/(6\ \text{kpc}) \qquad \text{(III.28)}$$

with r = 0.90. Then, the above halo/disk size relation suggests that in large galaxies the dissipational matter has collapsed to a a much larger extent than in the smaller ones. More precisely, the distribution of luminous matter encompasses a fraction of the total halo mass $M_{halo}(R_H)$ which scales as $M_{halo}^{-1/2}(R_H)$, so that by means of (III.27) and (III.28) we can predict an upper limit to the disk radius: $R_{25} \leq 200$ kpc. As a comparison, the largest identified spiral galaxy (Romanshin 1983), UGC 2885, has $R_{25} \simeq 120$ kpc.

The slope of the density/halo correlation matches that of the spatial covariance function $\xi(R)$ found for field galaxies.(a review in Fall, 1979). Then, this implies the existence of a correlation function in density space, defined accordingly to the spatial covariance function, of the form $\eta(\rho) \propto \rho$. From (III.27) it follows:

$$\rho(R)/\rho_{cr} = \xi(R) = 20\ R^{-1.8} \qquad \text{(III.28)}$$

where R is in Mpc, $\rho_{cr} = 4.8\ 10^{-30}$ g cm^{-3} and the ratio ρ/ρ_{cr} is H_o-independent.

This result supports the hierarchical clustering scenario: on all scales from the individual galaxies to superclusters, $\xi(r)$ has the same functional power-law form.

VII CONCLUSIONS.

Using an analytical treatment in the framework of the disk-halo model, we show that the kinematics of spiral galaxies reveals a strong imprint of the individual integral properties of dark and luminous mass components. we find that the shape of the rotation curves is determined by the disk/halo mass ratio. As indicated by its trends with luminosity, mass, optical size there is not preferred value in the disk/halo mass ratio. It spans a very broad range of values, being approximately proportional to the luminosity.

Correcting the total circular velocity for the halo's dynamical contribution we can couple the disk-related dynamics to the luminosity and to the optical radius. Then, we theoretically justify the 'empirical' Tully-Fisher relation as the realization of the centrifugal equilibrium of a self-gravitating disk embedded in a spherical halo. This enables us to work out, taking into account the different contribution of dark matter to dynamics along the luminosity sequence, a significantly better physical relation involving the disk contribution to the total velocity.

Furthermore, a disk velocity/(optical radius) relation shows that the disk rotation frequency at the isophotal radius is essentially the same for all spiral galaxies regardless their luminosity, sizes and morphological types.

Therefore, halo properties are worked out. we find that integral halo properties correlate with the disk ones, strongly supporting the view that a dynamical coupling between the proto-halo and the infalling baryonic matter modelled the present structure of galaxies.

Moreover, we are able to investigate the auto-correlation function for dark halos. We find that it closely follows the galaxy-galaxy correlation function so that a picture of hierarchical clustering naturally emerges.

Object	M_B	V_{MAX}	$\tilde{V}$	R_{25}	V_1	V_o
N2998	−22. 29	210. 0	52. 4	40. 0	43. 6	185. 0
N801	−23. 31	224. 0	67. 9	53. 8	−23. 2	226. 0
N3495	−21. 31	175. 0	22. 3	15. 5	113. 0	84. 2
N1421	−22. 15	196. 0	28. 3	17. 6	100. 0	105. 3
N2608	−20. 74	120. 0	18. 95	15. 2	76. 2	72. 7
N2742	−20. 54	173. 0	31. 5	12. 6	76. 1	116. 0
N4062	−19. 5	162. 0	26. 0	9. 0	71. 5	95. 8
N1035	−19. 69	133. 0	21. 9	7. 6	59. 0	80. 6
N3672	−21. 52	191. 0	49. 9	18. 7	21. 2	174. 1
N4682	−20. 05	173. 0	38. 9	17. 5	44. 9	139. 0
IC467	−21. 35	149. 0	31. 8	21. 5	40. 9	114. 0
N7541	−22. 30	245. 0	39. 8	28. 5	130. 0	148. 0
N4321	−21. 53	212. 0	50. 1	20. 1	44. 7	177. 7
N753	−22. 47	212. 0	56. 1	44. 7	34. 8	197. 0
U3671	−20. 96	134. 0	18. 1	16. 8	69. 4	67. 6
N1087	−21. 30	148. 0	25. 3	15. 6	63. 8	93. 2
N4605	−18. 59	93. 0	8. 3	4. 4	86. 8	32. 0
N2715	−21. 21	161. 0	30. 3	20. 4	49. 0	109. 2
N7664	−21. 69	201. 0	46. 0	34. 7	60. 0	165. 0
N701	−20. 51	149. 0	16. 15	12. 9	179. 5	51. 5
N3054	−21. 63	255.	51. 77	25. 7	77. 4	186. 8
N7537	−21. 23	142.	40. 4	18. 3	−0. 7	138. 0
N1515	−20. 72	231.	50. 2	13. 6	−57. 3	197. 5
N7119	−22. 0	258.	74. 6	26. 5	17. 3	266. 0
N7606	−22. 34	220.	87. 2	39. 0	−46. 0	208. 0
N3200	−22. 07	205.	71. 0	46. 0	36. 3	251. 4
U12810	−23. 06	230.	98. 1	51. 8	30. 0	204. 0
N3145	−22. 98	270.	63. 3	31. 8	66. 1	226. 0
N1620	−22. 06	248.	43. 9	29. 8	117. 8	161. 8
N1085	−22. 80	314.	89. 33	34. 0	5. 0	305. 0
U11810	−21. 4	187.	39. 2	34. 0	65. 8	142. 1
N7171	−21. 25	213.	56. 3	23. 9	29. 5	197. 3
N4448	−20. 1	190.	36. 83	11. 0	104. 0	136. 0
N1325	−20. 87	184.	30. 41	18. 8	78. 8	112. 9
N3223	−22. 64	254.	67. 82	34. 8	20. 3	236. 6
N7083	−22. 3	272.	63. 0	39. 0	0. 0	214. 0
N2708	−20. 6	241.	36. 2	14. 7	157. 3	136. 0
N2590	−21. 9	252.	54. 4	39. 6	107. 0	198. 0
N1417	−22. 28	328.	67. 4	33. 7	86. 6	242. 0
N3067	−20. 30	150.	30. 9	9. 6	53. 3	108. 9
N3792	−21. 7	273. 0	60. 0	24. 6	0. 0	273. 0
N5426	−21. 24	157. 5	46. 1	20. 3	0. 0	157. 5
N4565	−23. 0	254.	74. 4	46. 6	0. 0	254. 0
N5383	−22. 5	219.	65. 7	22. 0	−14. 0	221. 0
N7331	−22. 4	240.	57. 7	34. 1	13. 0	213. 0
N5033	−21. 3	210.	54. 3	20.	20. 0	171. 5
N2336	−22. 5	251.	71.4	46. 2	6. 0	245.
N5643	−21. 21	330.	47. 0	15. 7	160.	175.
N7339	−20. 54	160.	38. 9	12. 0	27.	137.
N5905	−22. 32	249.	61. 6	41. 3	27.	215.
165	−22.	160.	41. 1	40. 9	3.	145.
N4254	−21. 51	210.	41. 6	15. 6	60.	150.
N4654	−20. 77	200.	23. 7	13.	169.	90.
N3769	−22. 32	175.	90. 9	27. 0	9.	172. 5
N3877	−21. 61	230.	32. 1	26. 4	30.	200.
N5371	−21. 45	134.	25. 2	16. 1	22.	104.
U10795	−23. 50	250.	64. 4	11. 4	0.	220.
N4170	−21. 24	190.	43. 9	22. 4	0.	190.
N3526	−19. 40	150.	27. 5	6. 2	50.	100.

TABLE 6

The Sample B.

Object	M_B	V_{MAX}	$\widetilde{V}$	R_{25}	V_1	V_o	R_B	$I(0)$	R_D	$B-V$
N2998	−22.79	213.0	52.4	40.0	43.6	185.0	7.0	20.2	8.3	.5
N4605	−18.59	93.	8.3	4.4	86.8	32.	1.5	20.6	1.0	.5
N801	−23.31	224.0	67.9	50.8	−23.2	226.0	9.0	20.9	13.0	.5
N3495	−21.31	175.0	25.3	15.5	113.0	84.2	4.0	21.3	4.9	.54
N1421	−22.15	196.0	20.3	19.6	100.0	105.3	7.0	22.5	8.3	.2
N2608	−20.74	120.0	10.95	15.2	76.2	72.7	4.0	19.5	3.0	.4
N2742	−20.54	173.0	31.5	13.6	76.1	116.0	3.0	21.5	3.8	.4
N4062	−19.5	162.0	26.9	9.0	71.5	95.8	0.5	23.0	4.1	.6
N1035	−19.69	133.0	21.9	7.6	59.0	80.6	2.0	21.8	2.3	.6
IC467	−21.35	149.0	31.8	21.5	40.9	114.0	6.0	20.2	4.7	.5
N1087	−21.30	148.0	25.3	15.6	60.8	93.2	4.0	21.4	4.6	.4
N3054	−21.63	255.	51.77	25.7	77.4	186.0	5.0	20.0	5.4	.4
N7537	−21.23	148.	40.4	16.3	−0.7	138.0	4.0	20.1	3.7	.4
N2815	−22.0	292.	74.6	25.5	17.5	266.0	6.0	21.7	9.7	.7
N7606	−22.54	273.	82.2	32.8	46.0	208.0	10.0	20.3	8.3	.5
N4700	−22.02	245.	71.0	16.0	35.3	291.4	10.0	21.0	14.0	.6
N4910	−20.06	200.	30.1	21.8	30.0	204.0	16.0	20.3	11.2	.7
N7690	−22.06	300.	63.2	22.8	117.0	161.8	4.0	21.4	8.9	.6
N1085	−22.80	314.	89.33	34.6	5.0	305.0	8.0	21.5	10.0	.7
N3325	−20.87	184.	30.41	13.8	90.8	112.9	4.0	21.8	5.7	.5
N2708	−20.6	241.	36.2	14.7	157.3	136.0	4.0	21.5	4.3	.7
N1417	−22.20	320.	67.4	33.7	86.6	242.0	1.5	20.5	8.0	.7
N3067	−20.30	150.	30.0	9.6	53.3	108.9	3.0	22.1	3.3	.5
N5290	−21.61	230.	57.1	26.4	30.	200.	10.2	20.2	5.5	.5
N4682	−20.85	173.0	30.9	17.5	44.9	139.0	5.0	21.2	4.8	.5
N7541	−22.30	245.0	39.8	29.5	130.0	148.0	6.0	21.3	9.7	.6
N4321	−21.53	212.0	50.1	20.1	44.7	177.7	5.0	21.9	6.9	.6
N2715	−21.21	161.0	30.3	20.4	49.0	109.2	3.0	23.6	8.9	.4
N7171	−21.25	213	56.3	23.9	29.5	197.3	5.0	20.9	7.4	.6
N5383	−22.5	215.	65.7	30.0	−14.0	221.0	8.0	21.3	6.	.6
N7331	−22.4	240	57.7	34.1	13.0	213.0	12.0	22.0	10.6	.6
N5033	−21.3	210.	54.3	30	20.0	191.5	10.0	22.3	12.	.7
N2336	−22.5	251.	71.4	46.2	6.0	245.	13.3	21.8	15.8	.5
N5905	−22.32	245.	61.6	41.3	27.	215.	16.2	22.2	16.4	.5
N4254	−21.51	210.	41.6	15.6	60.	150.	1.9	21.0	4.4	.5
N3953	−22.37	172.	50.2	27.8	5.	172.5	9.9	20.9	7.4	.6
N4565	−23.0	254.	74.4	46.6	0.0	254.0	7.0	22.4	19.2	.6
N3992	−21.7	273.	60.	24.6	25.	248.	9.7	22.1	8.8	.7
N5426	−21.24	157.	46.1	20.3	0.	157.	5.0	22.1	6.3	.5
N3898	−20.5	252.	50.	14.7	72.	180.	1.0	23.1	7.	.6
N488	−22.52	405.	91.0	36.	80.	305.	2.0	21.0	10.4	.6
N2639	−21.9	350.	85.4	19.2	50.	300.	5.	19.3	3.2	.6
N3504	−20.75	107.	31.7	11.5	71.	116.	3.	22.4	4.8	.6

TABLE 7

The sample C.

Object	γ	$m_\odot / m_\odot$
N2998	1.080	0.185E+12
N4605	0.155	0.145E+10
N801	3.462	0.298E+12
N3495	0.438	0.354E+11
N1421	0.853	0.916E+11
N2608	0.381	0.160E+11
N2742	0.810	0.391E+11
N4062	1.332	0.373E+11
N1035	0.746	0.119E+11
IC467	0.902	0.422E+11
N1087	0.763	0.310E+11
N3054	0.812	0.137E+12
N7537	1.806	0.380E+11
N2815	3.459	0.337E+12
N7606	3.431	0.310E+12
N3200	2.389	0.522E+12
U12810	1.297	0.277E+12
N1620	0.752	0.186E+12
N1085	2.967	0.460E+12
N1325	0.642	0.620E+11
N2708	0.473	0.753E+11
N1417	0.995	0.311E+12
N3067	1.208	0.281E+11
N5290	1.246	0.135E+12
N4682	1.199	0.584E+11
N7541	0.722	0.186E+12
N4321	2.000	0.134E+12
N2715	2.114	0.860E+11
N7171	2.176	0.160E+12
N5383	3.631	0.134E+12
N7331	2.294	0.233E+12
N5033	6.741	0.266E+12
N2336	4.602	0.484E+12
N5905	4.460	0.449E+12
N4254	1.110	0.656E+11
N3963	2.332	0.110E+12
N4565	3.087	0.413E+12
N3992	1.920	0.253E+12
N5426	3.897	0.760E+11
N3898	3.079	0.192E+12
N488	1.750	0.620E+12
N2639	1.066	0.212E+12
N3504	1.351	0.549E+11

TABLE 8

Disk masses and ratios between the disk and halo contribution to V_{25}.

object	M_B	V_{25}	$\bar{V}$	R_{25}	K_{25}/R_0	$\bar{\beta}$
NGC 2998	-22.79	213	52.4	40.0	4.82	0.62
NGC 801	-23.31	224	67.9	53.8	4.14	0.85
NGC 3495	-21.31	175	22.3	15.5	3.16	0.26
NGC 1421	-22.15	196	28.3	19.6	2.36	0.32
NGC 2608	-20.74	120	19.0	15.2	5.07	0.32
NGC 2742	-20.54	173	31.5	12.6	3.32	0.45
NGC 4062	-19.50	162	26.0	9.0	2.19	0.37
NGC 1035	-19.69	133	21.9	7.6	3.30	0.39
IC 467	-21.35	149	31.8	21.5	4.57	0.52
NGC 1087	-21.30	148	25.3	15.6	3.39	0.41
NGC 3054	-21.63	255	51.8	25.7	4.76	0.48
NGC 7537	-21.23	142	40.4	18.3	4.95	0.74
NGC 2815	-22.00	292	74.6	26.5	2.88	0.71
NGC 7606	-22.54	273	87.7	39.8	4.80	0.87
NGC 3200	-22.87	285	71.8	46.0	3.11	0.71
NGC 12810	-23.06	238	58.1	51.8	4.63	0.62
NGC 1620	-22.06	248	43.9	29.8	3.35	0.43
NGC 1085	-22.88	314	89.3	34.8	3.48	0.82
NGC 1325	-20.87	184	30.4	18.8	3.30	0.39
NGC 2708	-20.60	241	36.2	14.7	3.42	0.34
NGC 1417	-22.28	328	67.4	33.7	4.21	0.51
NGC 3067	-20.33	150	30.0	9.6	2.91	0.53
NGC 5290	-21.61	230	57.1	26.4	4.80	0.63
NGC 4682	-20.85	173	38.9	17.5	3.65	0.60
NGC 7541	-22.30	245	39.8	28.5	2.94	0.39
NGC 4321	-21.53	212	50.1	20.1	2.91	0.66
NGC 2715	-21.21	161	30.3	20.4	2.29	0.46
NGC 7171	-21.25	213	56.3	23.9	3.23	0.76
NGC 5383	-22.50	215	65.7	22.0	3.67	0.89
NGC 7331	-22.40	240	57.7	34.1	3.22	0.68
NGC 5033	-21.30	218	54.3	28.0	2.33	0.65
NGC 2336	-22.50	251	71.4	46.2	2.92	0.82
NGC 5905	-22.32	245	61.6	41.3	2.52	0.68
NGC 4254	-21.51	210	41.6	15.6	3.55	0.51
NGC 3963	-22.37	172	50.2	27.8	3.76	0.83
NGC 4565	-23.00	254	74.4	46.6	3.53	0.84
NGC 3992	-21.70	273	60.0	24.6	2.80	0.58
NGC 5426	-21.24	157	46.1	20.3	3.22	0.86
NGC 3898	-20.50	252	50.0	14.7	2.10	0.47
NGC 488	-22.52	405	91.0	36.0	3.46	0.61
NGC 2639	-21.90	350	85.4	19.2	6.00	0.56
NGC 3504	-20.75	187	31.7	11.5	2.40	0.40
NGC 4605	-18.59	93	8.3	4.4	4.40	0.10

TABLE 9

Disk to total mass ratios for Sample C. Basic kinematical and photometric properties are also inserted in order to show the trend of the scenario discussed in the text.

FIGURE CAPTIONS

Fig. 5 Comparison between the dynamical $\tilde{V}/V$ (decreasing curves) and the luminous one (increasing curves) along the galaxy disk. Galactocentric distances are in kpc.

Fig. 6 Values of β as a function of $\tilde{V}/V$ for galaxies belonging to sample C.

Fig. 7 Luminous masses vs dynamical disk mass for sample C. Note the very small scatter 0.2 dex and the slope significantly near to 1 .

Fig. 8 $\hat{\beta}$ as function of R_{25}/a for $\tilde{V}/V = .293$ (flat rotation curve) and $R_{25}/R_D = 3.6$ (average value for sample C). Note that the 1 σ uncertainty is less than 0.1 while the range induced by the variations of $\tilde{V}/V$ among galaxies is about 0.8.

Fig. 9 The luminosity/velocity correlation for sample C. The absolute blue magnitude is plotted vs the disk rotational velocity(top panel) and the total observed velocity (Tully-Fisher relation, bottom panel) respectively. Coupling the luminosity with the disk dynamics we obtain a sizable reduction of the scatter which affects the Tully-Fisher relation.

Fig. 10 Disk-halo mass ratios drive the steepness of the rotation curves of galaxies.

Fig 11 $(M/L)_D$ vs color for sample C. The drawn line is the theoretical relation for the case of continuous

star formation of Larson-Tinsley evolutionary models.

Fig. 12 The density/radius relation in halos. The density is averaged over the halo volume encompassed by the optical disk (top panel) and over the entire volume (bottom panel) derived by imposing that at the edge of the halo $M_T/M_D = 10$.

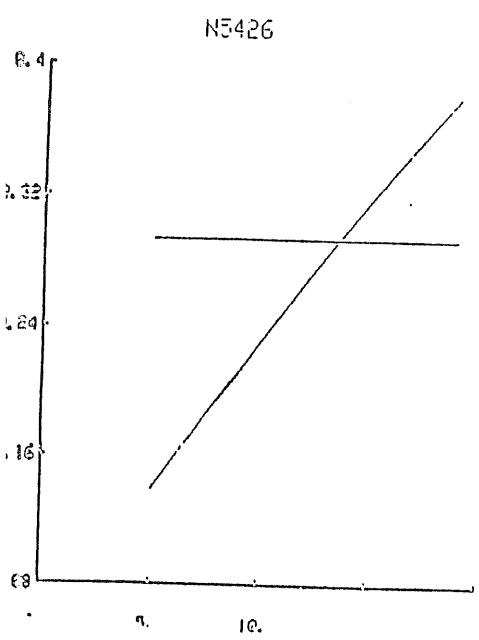

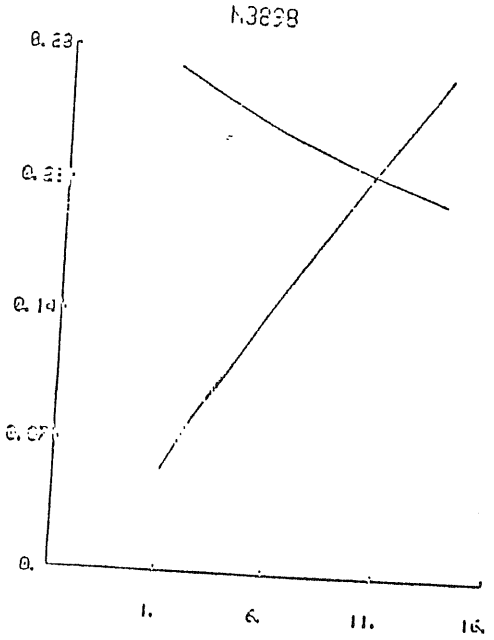

FIGURE 5

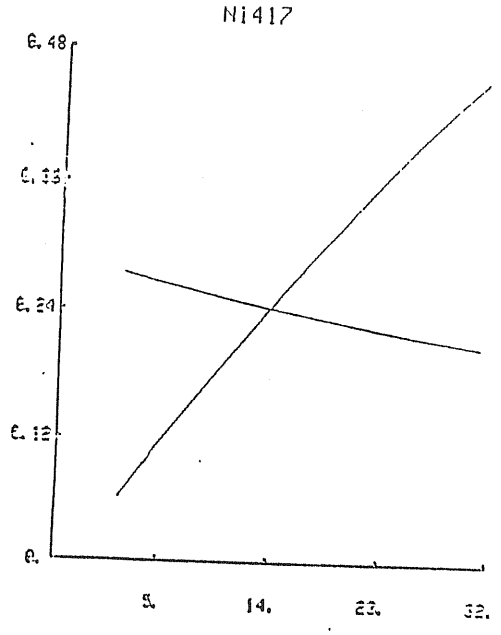
Ni417
0.48
0.36
0.24
0.12
0.
5.
14.
23.
32.

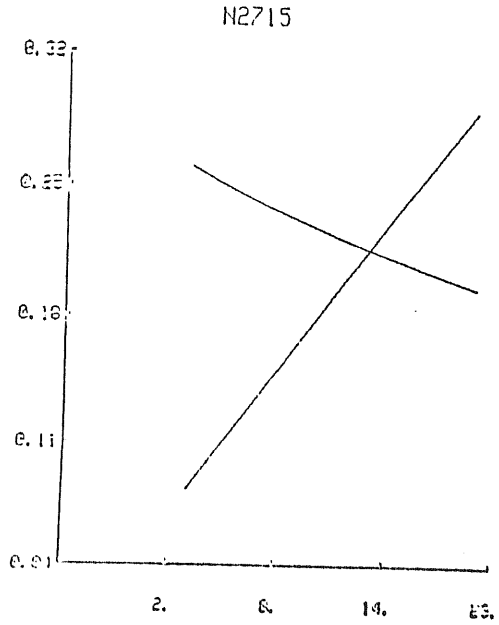
N2715
0.32
0.24
0.16
0.08
2.
8.
14.
20.

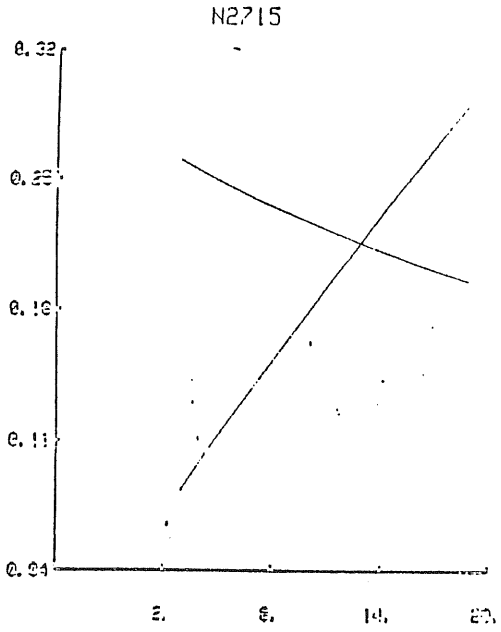
N2715
0.32
0.24
0.16
0.08
2.
8.
14.
20.

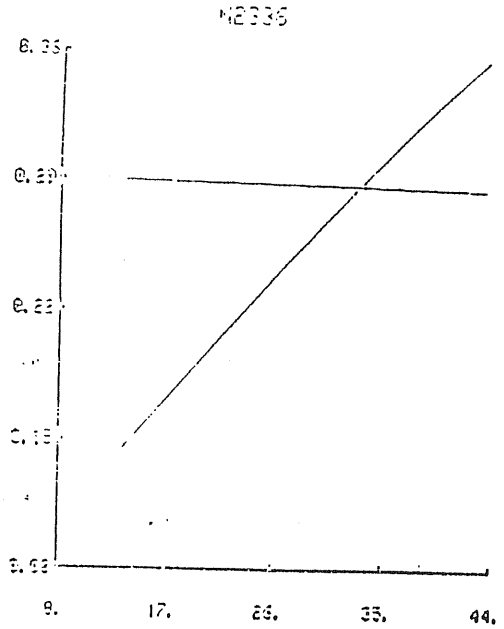
N2336
0.36
0.30
0.24
0.18
0.12
9.
17.
26.
35.
44.

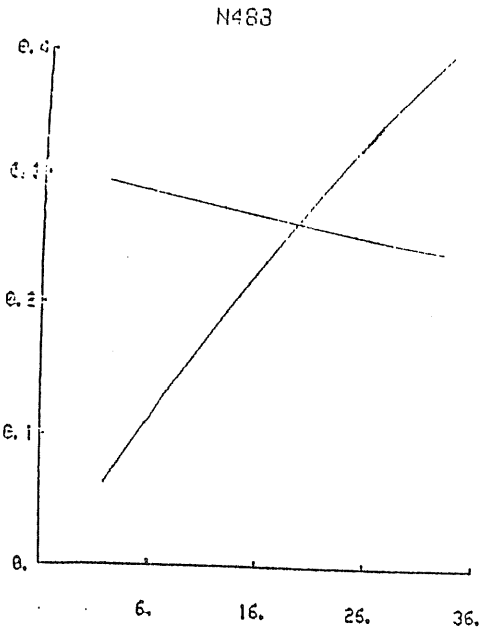
N483
0.4
0.3
0.2
0.1
0.
6.
16.
26.
36.

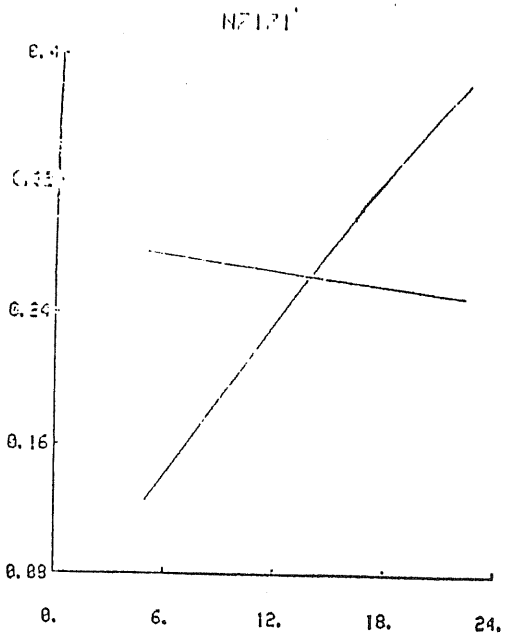
N2171
0.4
0.32
0.24
0.16
0.08
0.
6.
12.
18.
24.

N4062

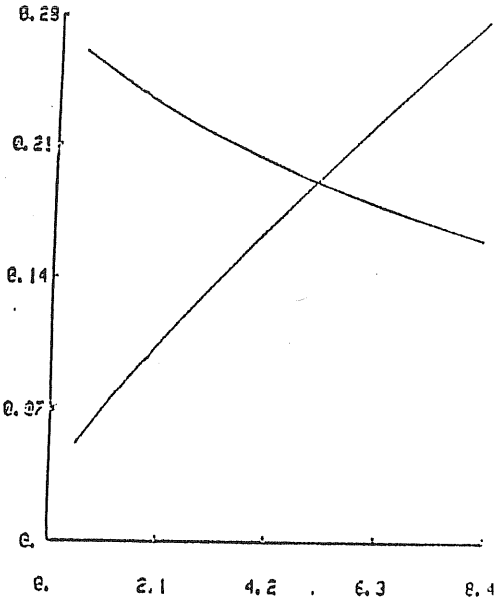

N7537

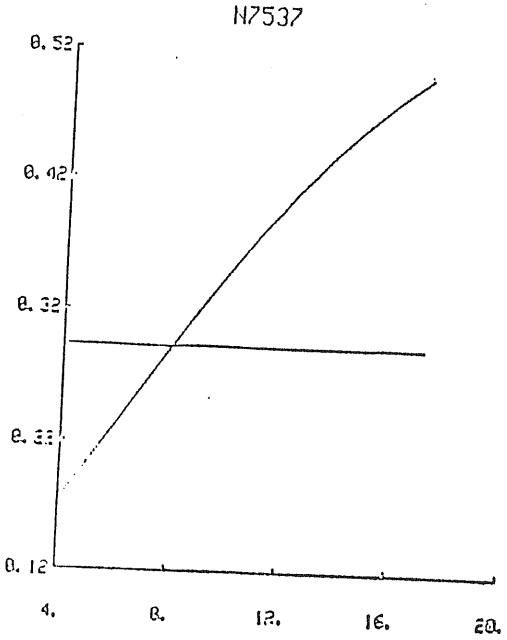

N1087

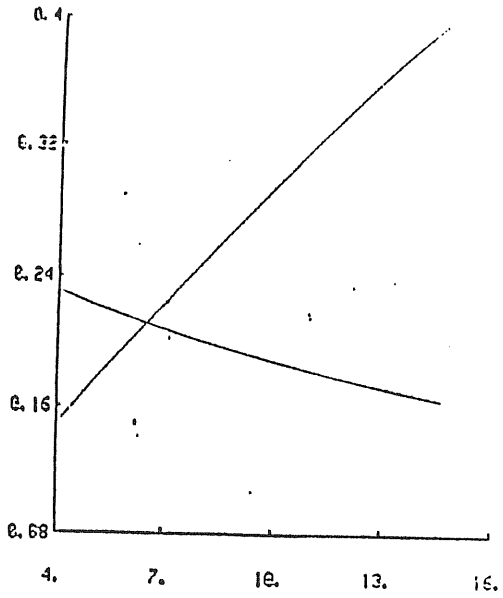

N7696

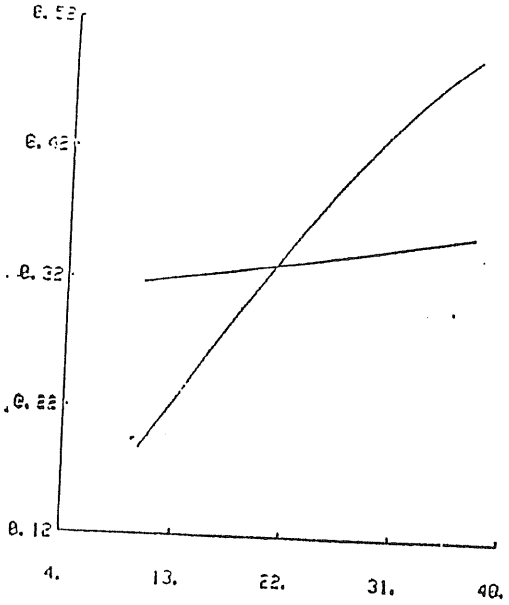

N2815

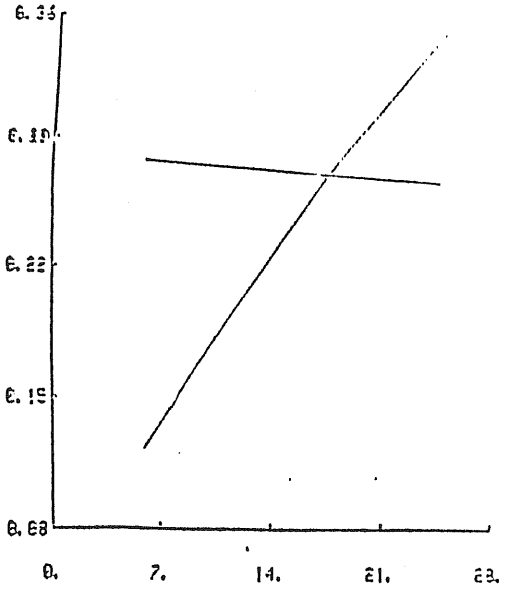

N5290

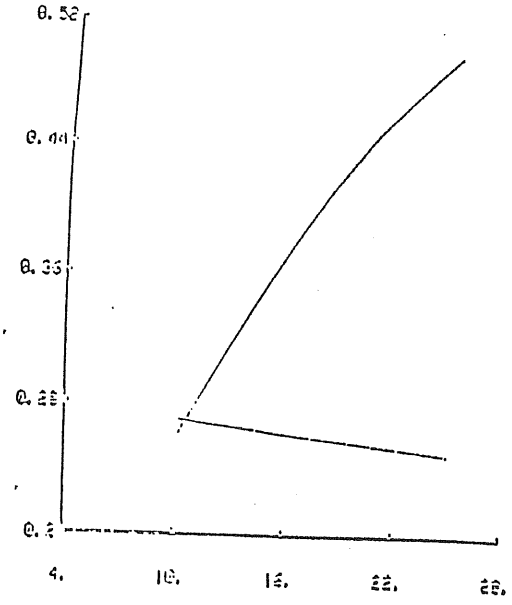

N1421

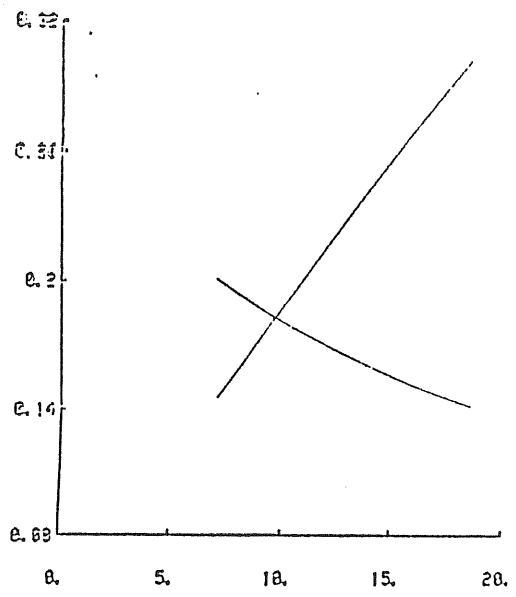

N3495

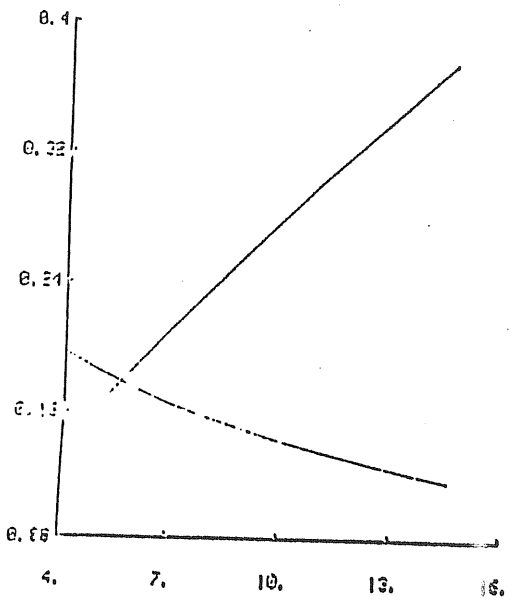

N2742

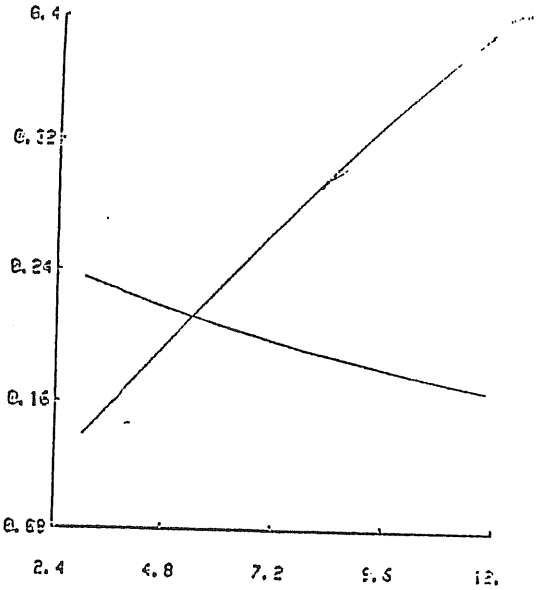

N2608

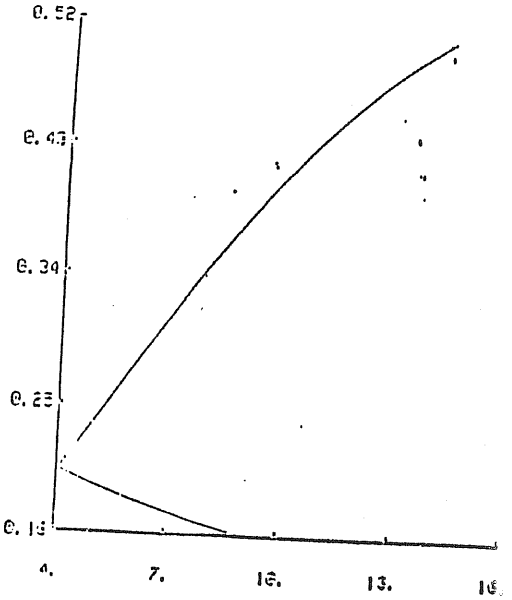

N1035

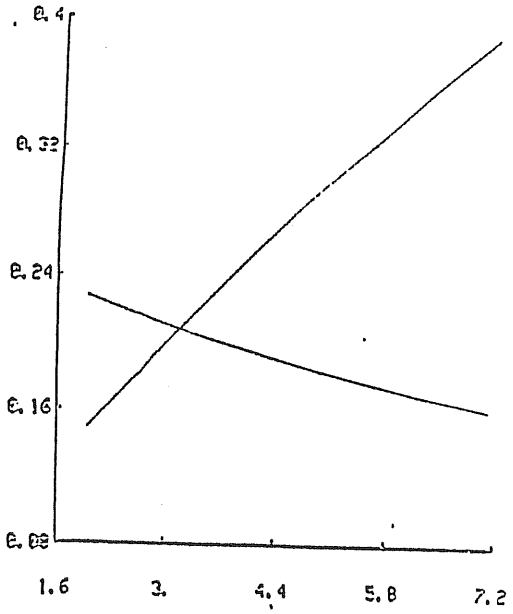

IC467

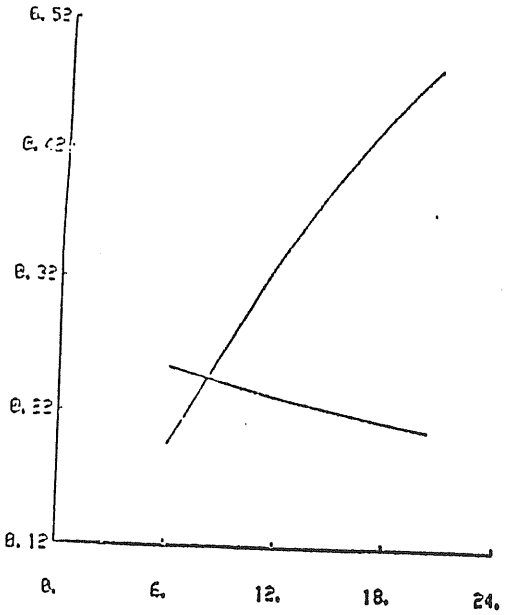

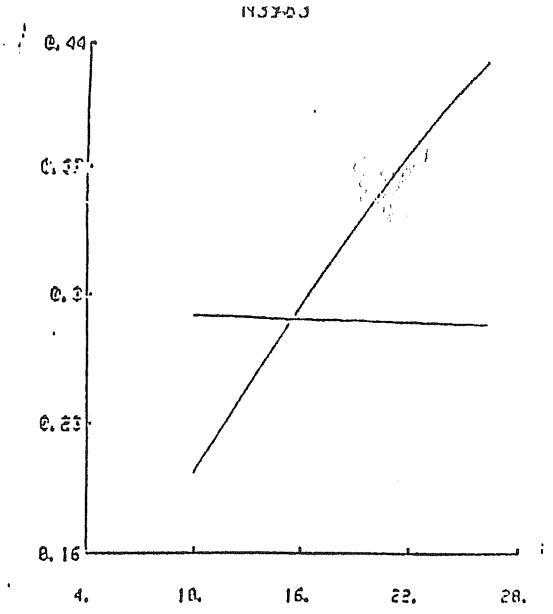

N5383

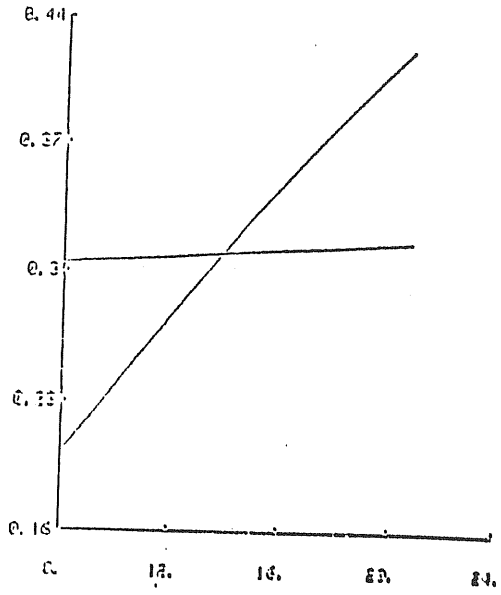

N3504

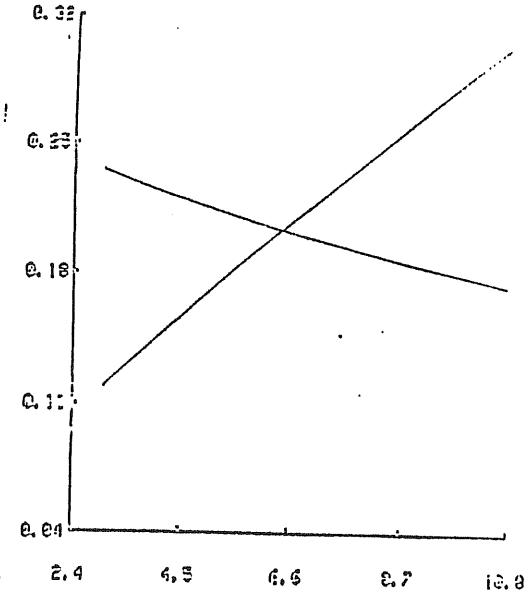

N1520

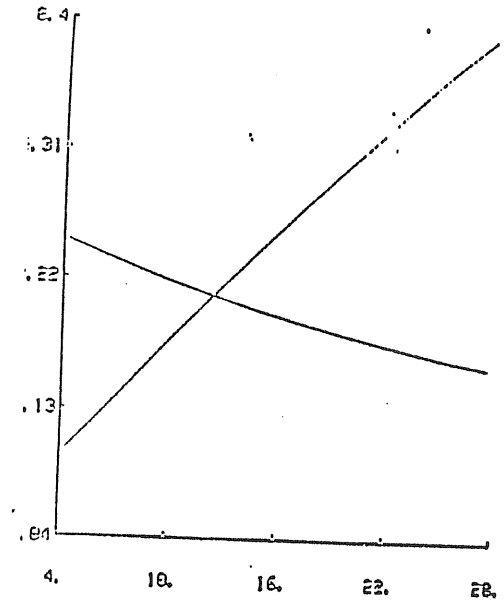

N2639

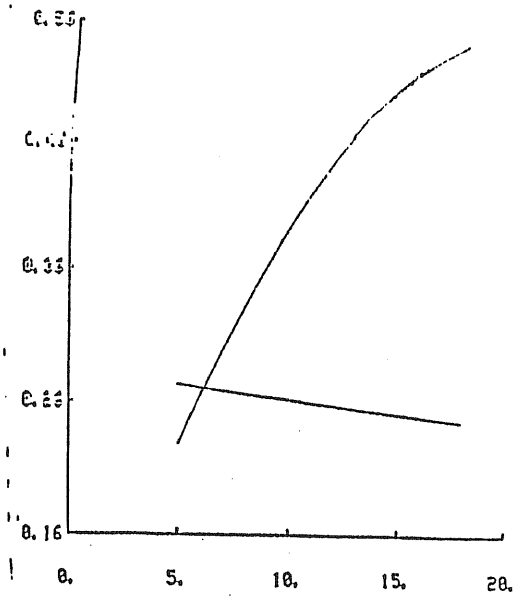

N1085

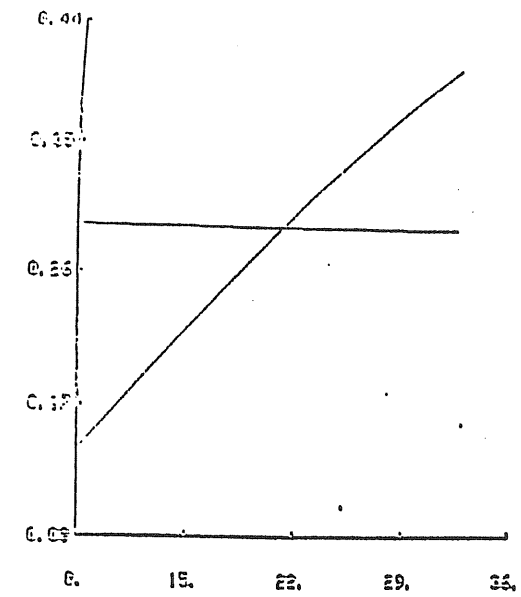

N3054

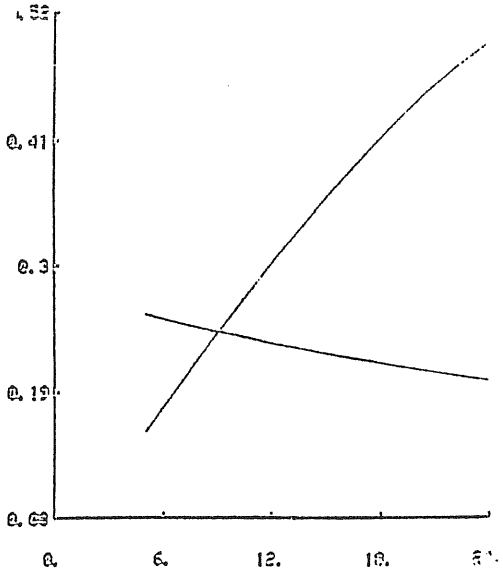

N5905

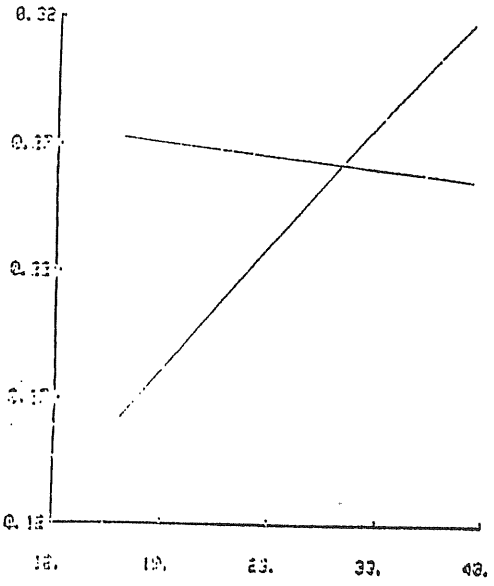

N3200

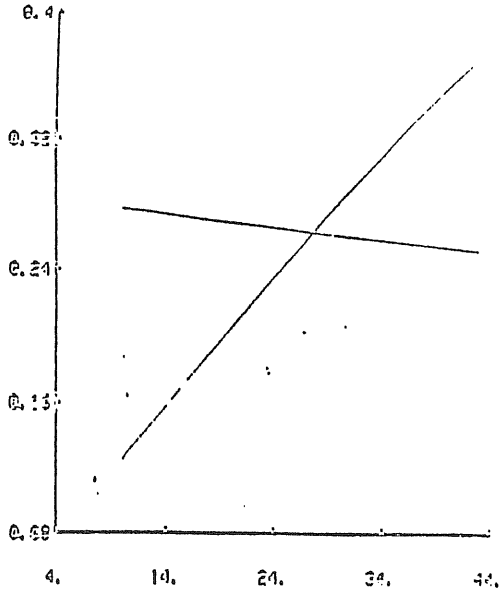

N5033

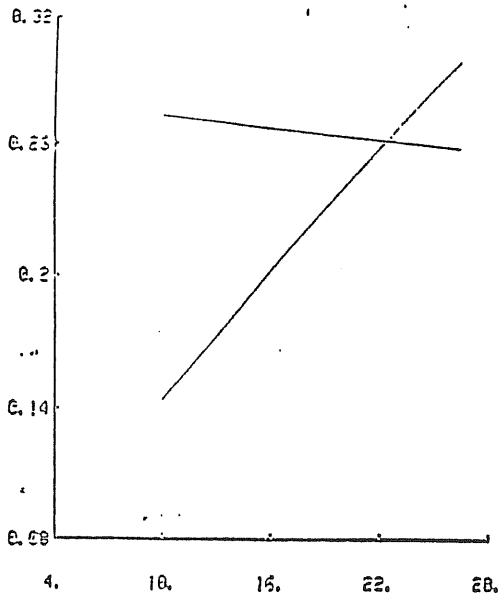

N5426

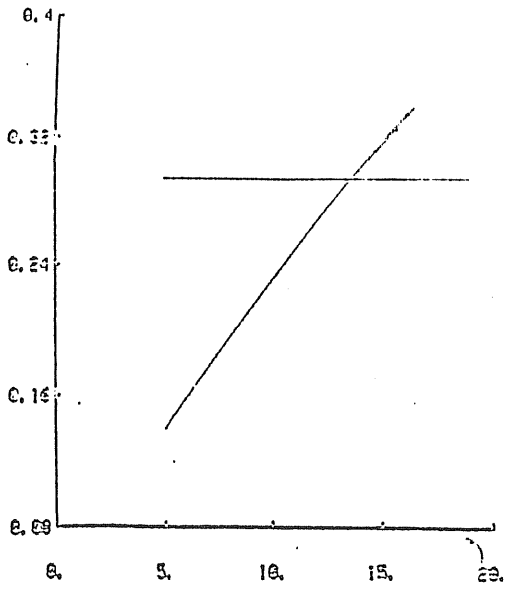

N801

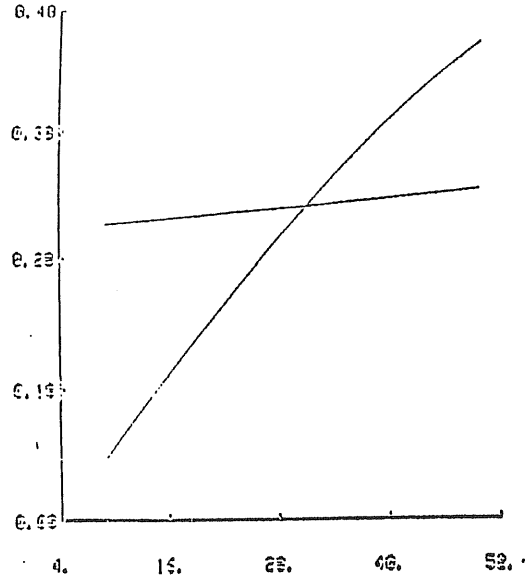

U 12810

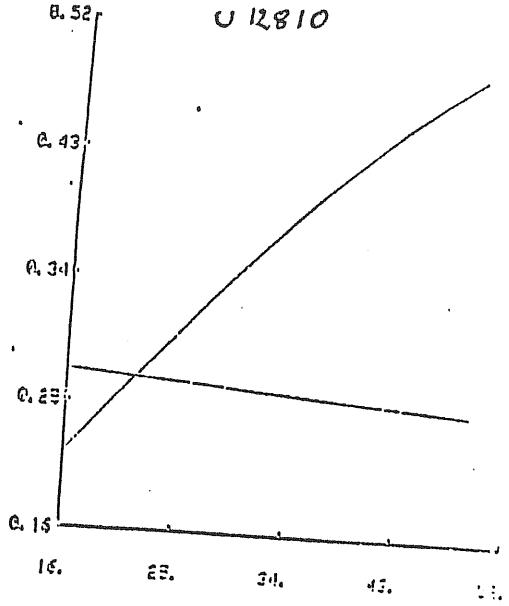

N1325

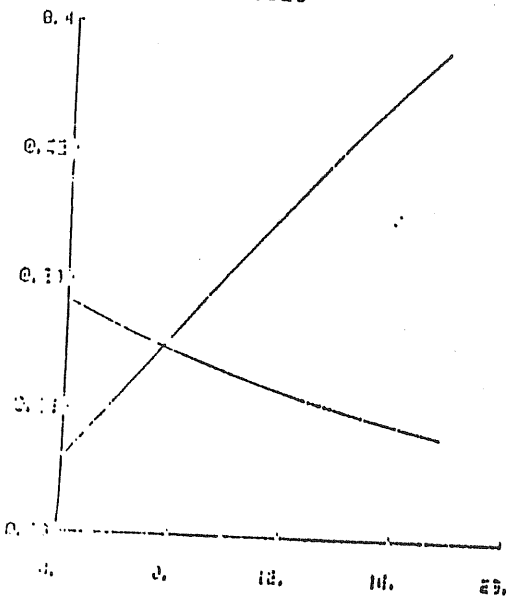

N4682

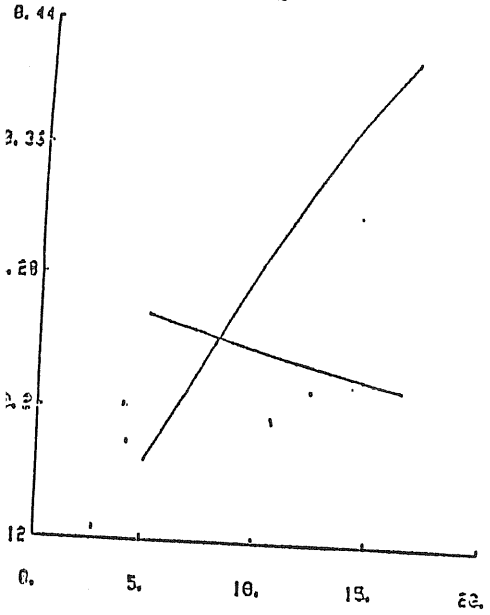

N4321

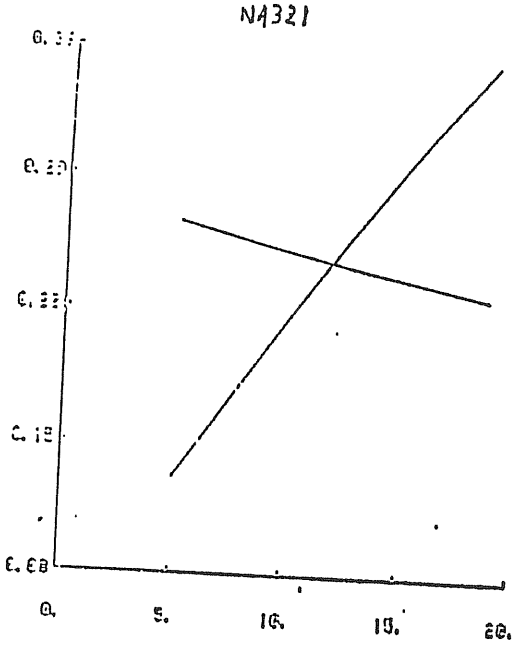

N7541

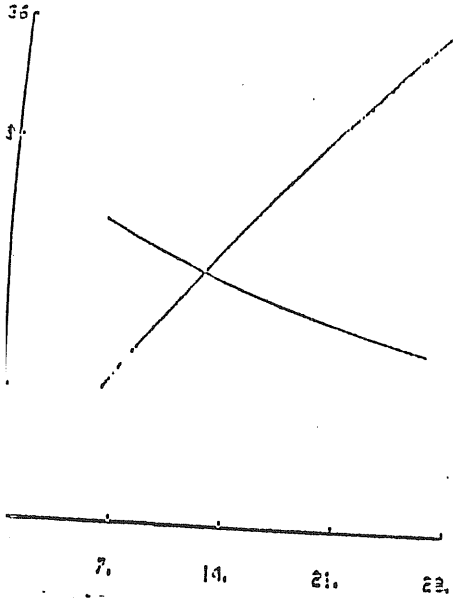

N3067

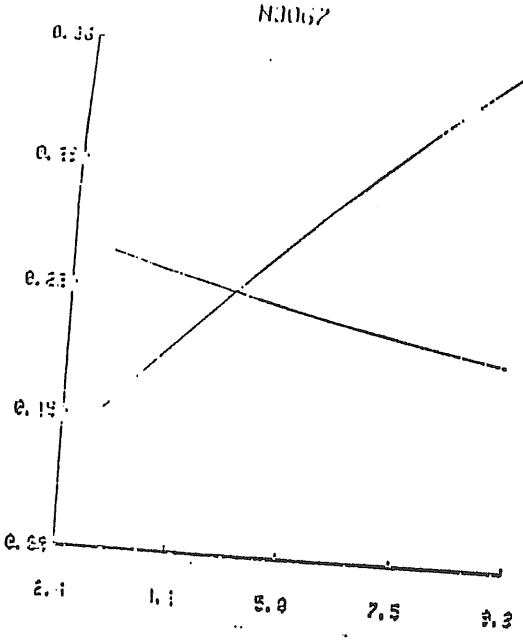

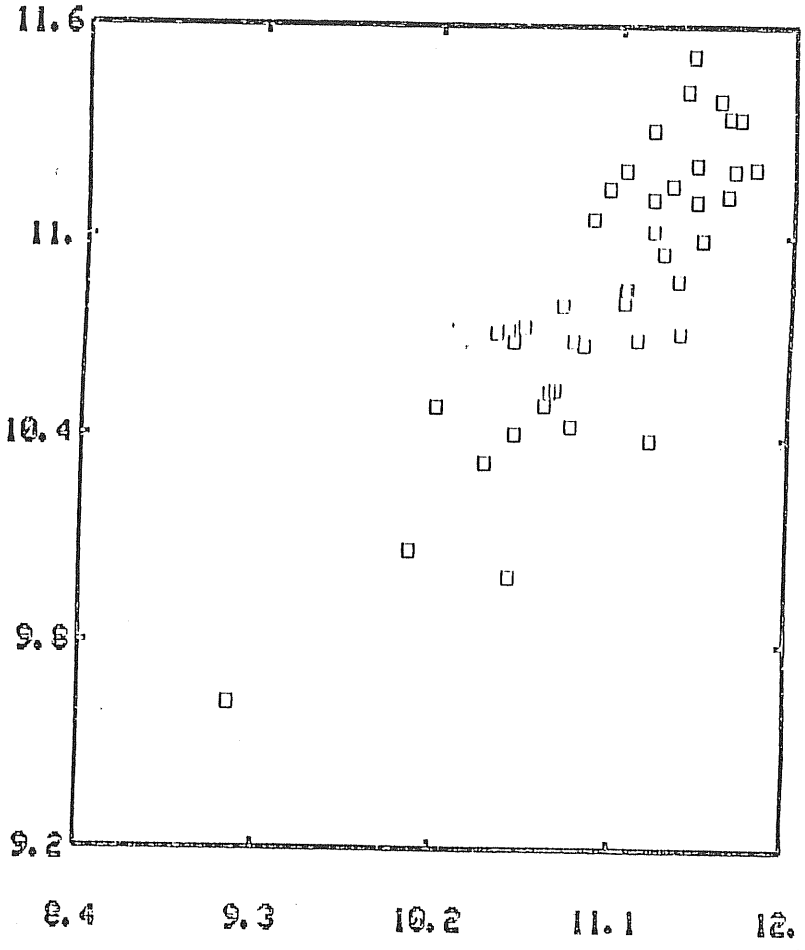

FIGURE 6

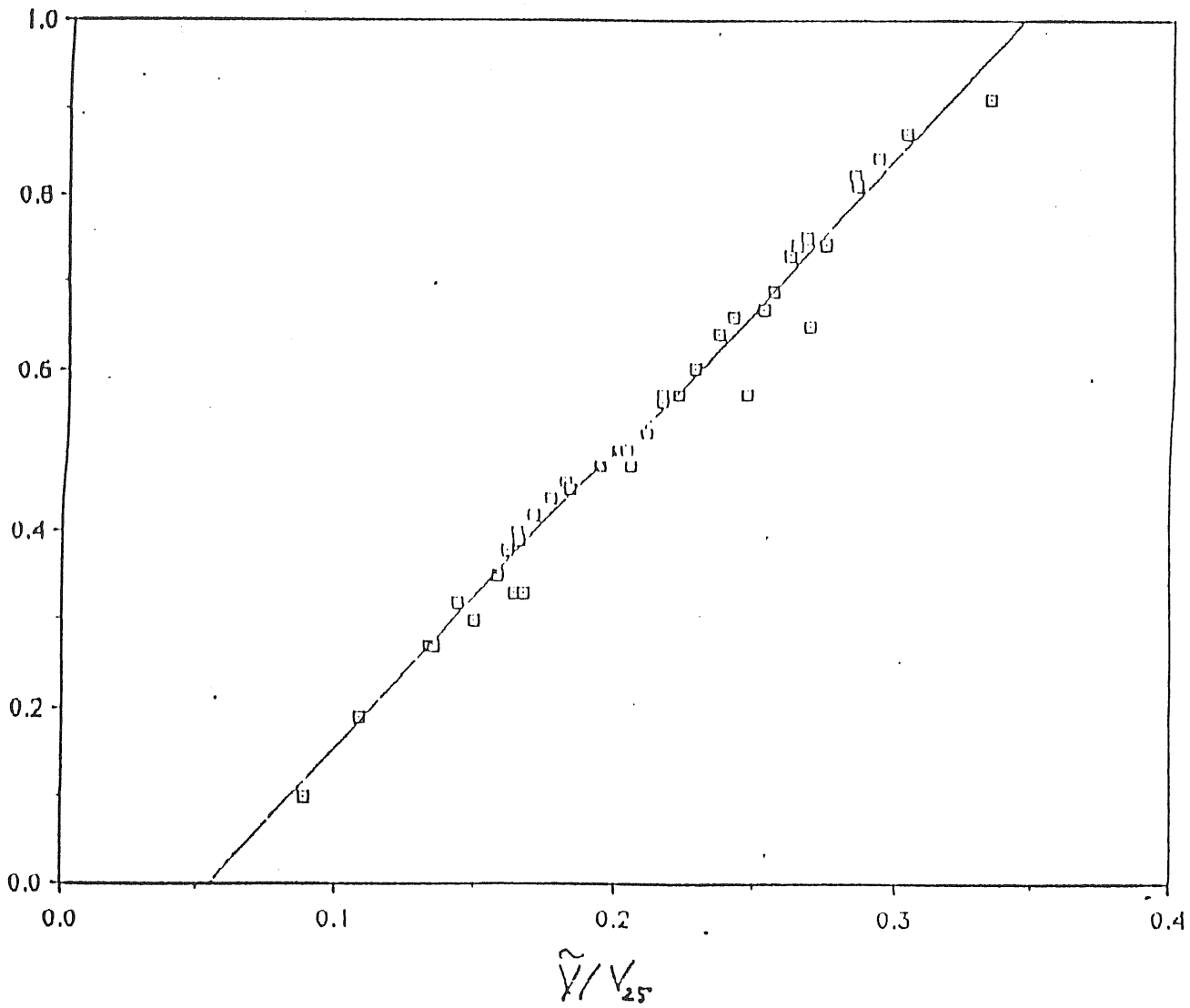

FIGURE 7

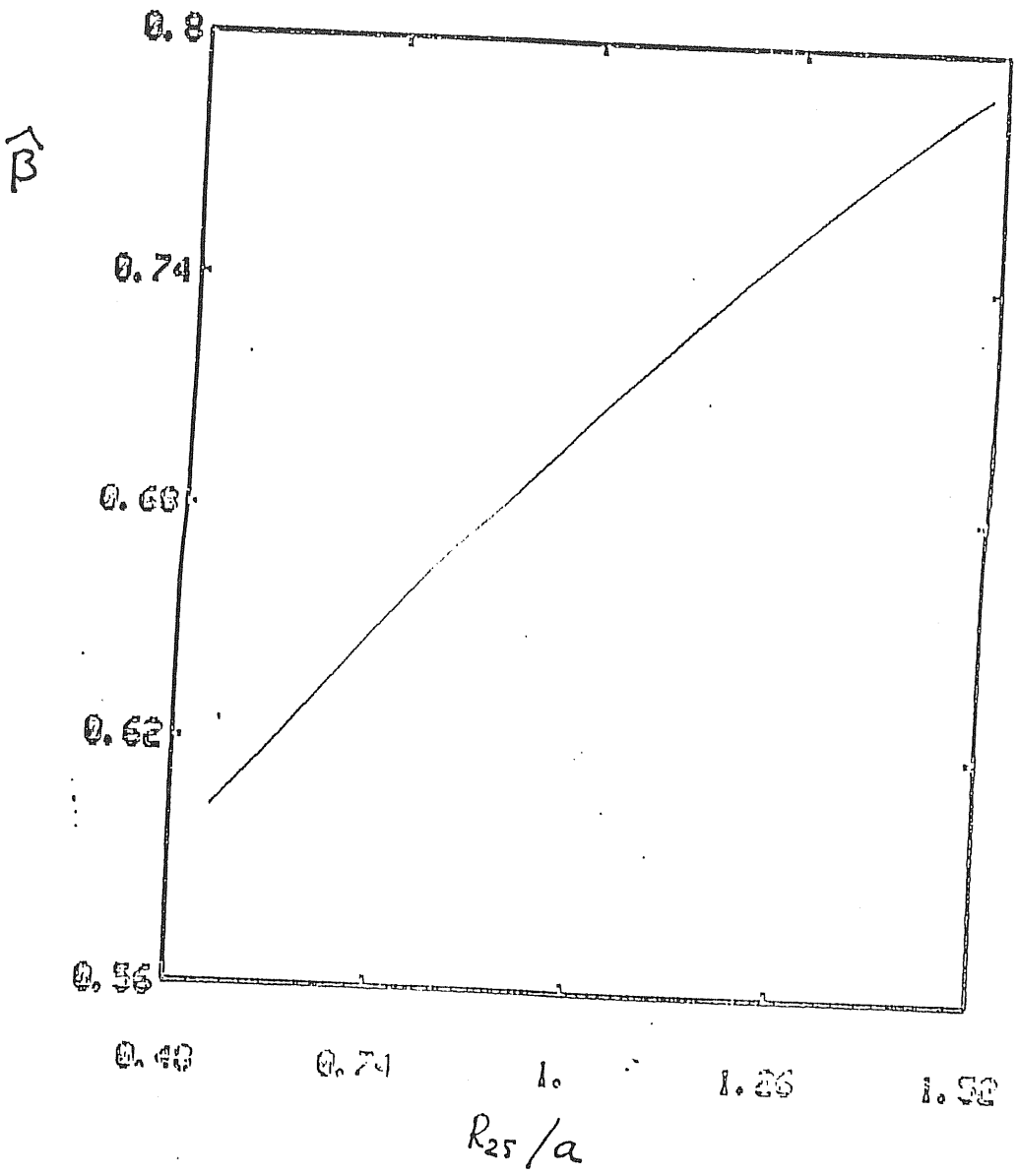

FIGURE 8

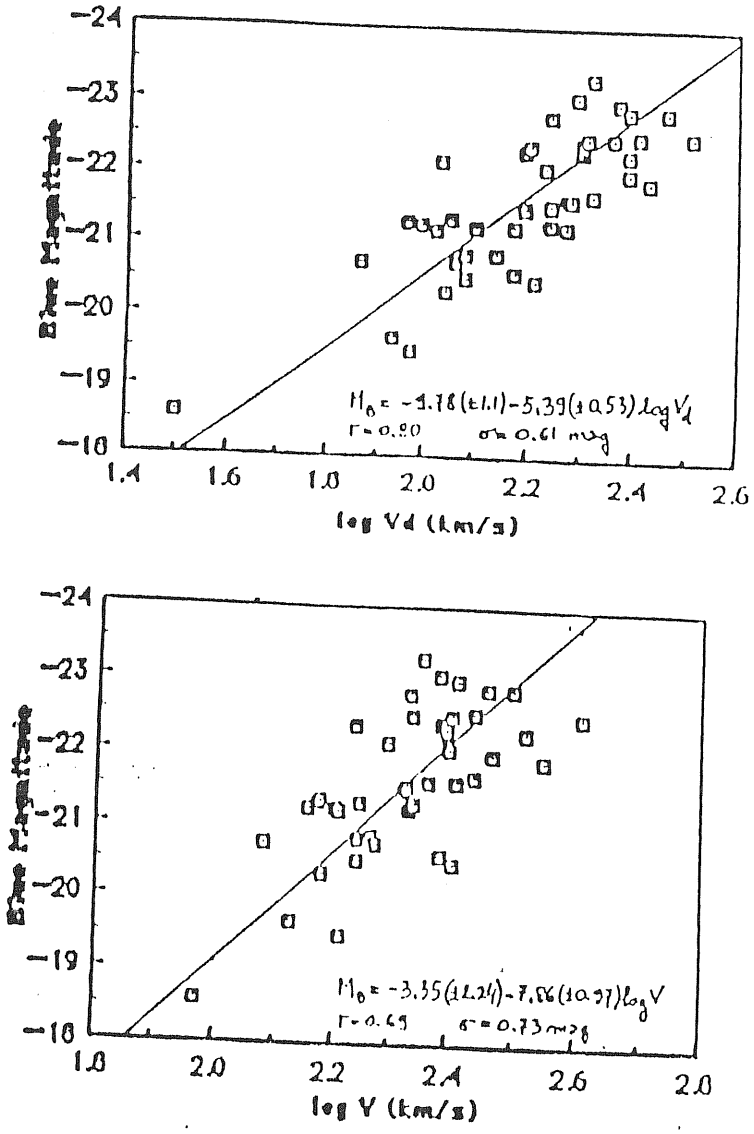
−24
−23
−22
−21
−20
−19
−18
Blue Magnitude
1.4
1.6
1.8
2.0
2.2
2.4
2.6
log Vd (km/s)
$M_0 = -1.78(\pm 1.1) - 5.39(\pm 0.53) \log V_d$
r = 0.80
σ = 0.61 mag

−24
−23
−22
−21
−20
−19
−18
Blue Magnitude
1.8
2.0
2.2
2.4
2.6
2.8
log V (km/s)
$M_0 = -3.35(\pm 1.24) - 7.86(\pm 0.97) \log V$
r = 0.69
σ = 0.73 mag

FIGURE 9

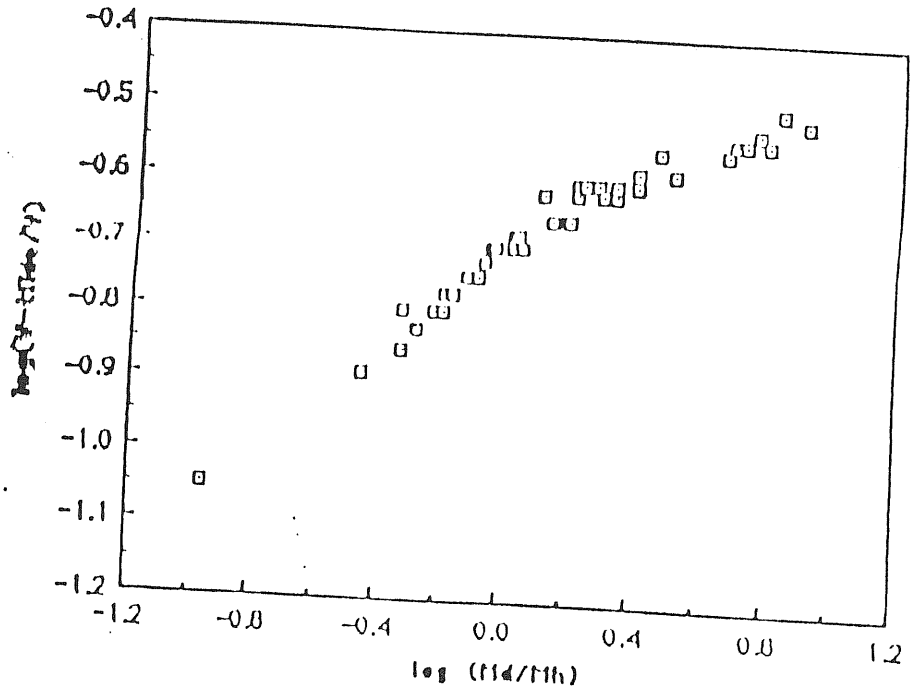

FIGURE 10

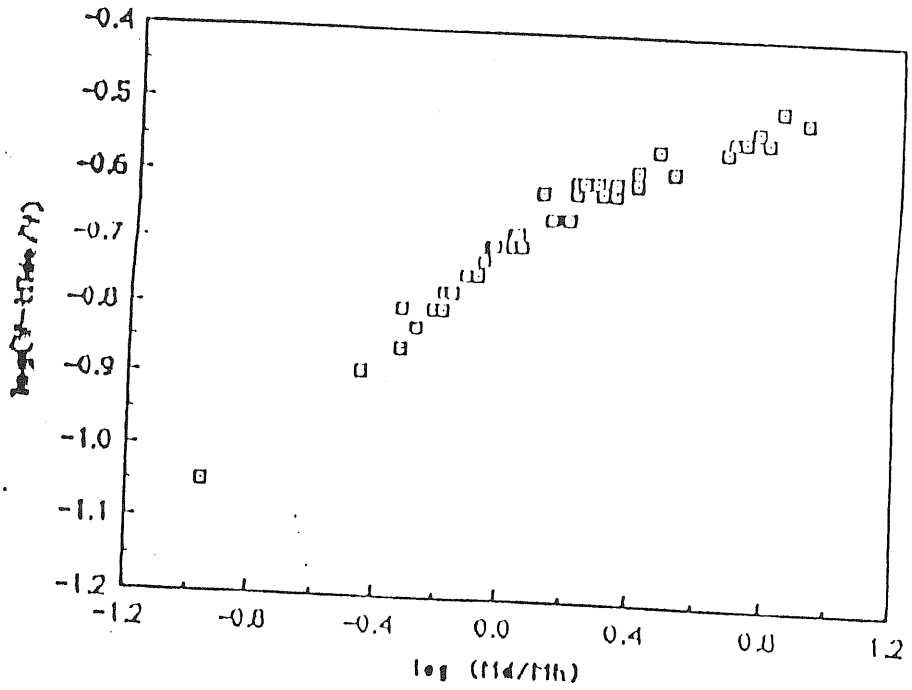

FIGURE 10

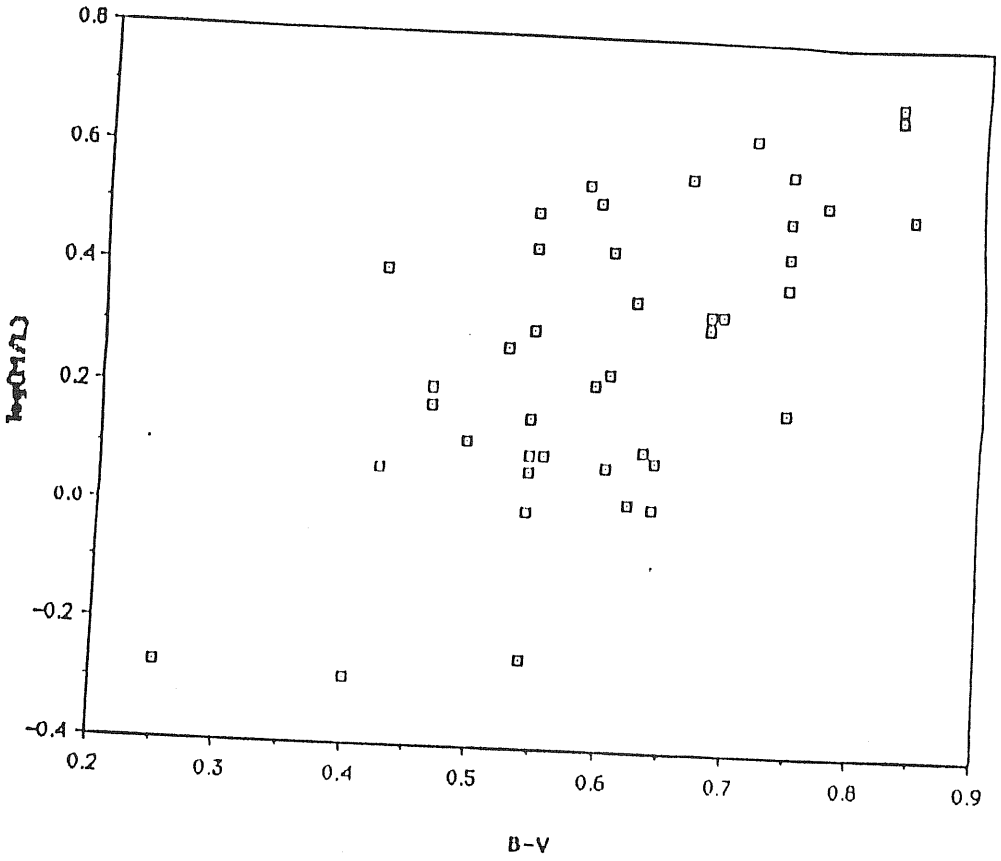

FIGURE 11

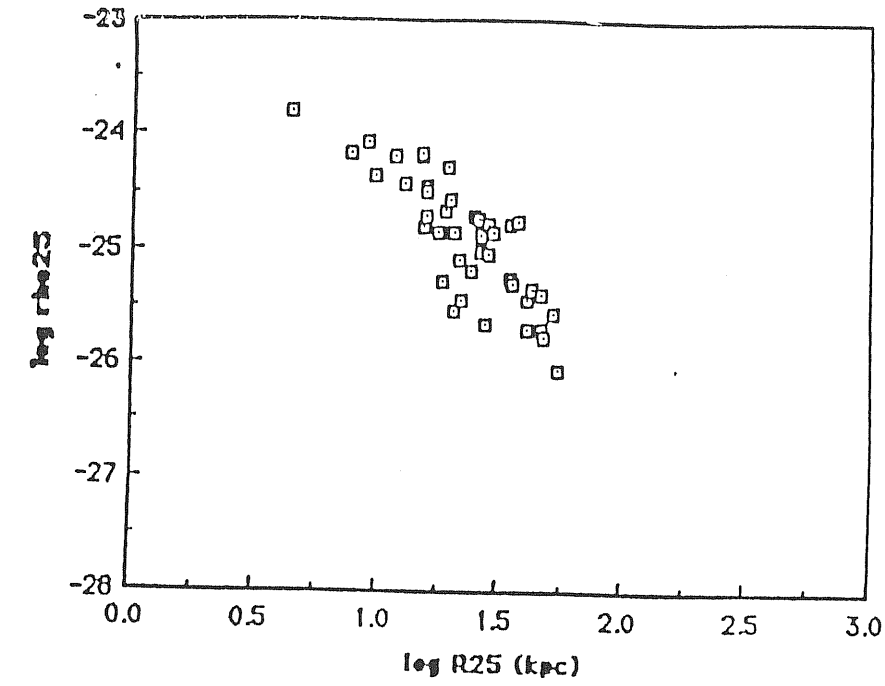
-23
-24
-25
-26
-27
-28
log re25
0.0
0.5
1.0
1.5
2.0
2.5
3.0
log R25 (kpc)

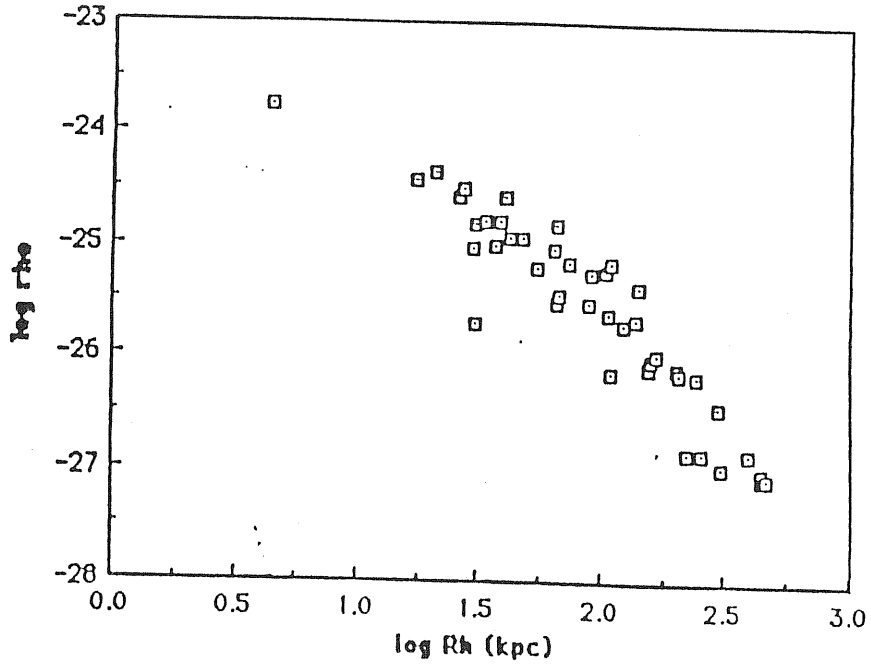
-23
-24
-25
-26
-27
-28
log re
0.0
0.5
1.0
1.5
2.0
2.5
3.0
log Rh (kpc)

FIGURE 12

CONCLUSIONS

In this thesis we have worked out from the observable quantities, the physically relevant ones in order to obtain the building blocks for spiral galaxy formation theory. The main new aspects of our strategy are:

1) we are interested in general properties of basic galactic quantities, then we consider very seriously **persistent** properties and neglect **occasional** ones;

2) we do not derive them, as very often is done in the literature, as a by-product of an analysis aimed to work out **local** and/or **irrelevant** (to the missing mass and disk formation issues) quantities, but we develop several methods whose target is really to obtain integral quantities with the minimum of assumptions made.

To this end, firstwhole, using all available data (59 galaxies with kinematics available and 43 also with photometry available) we organized the observational information (both kinematical and photometric) in a simple phenomenological scenario.

a) The individuality of each galaxy in its integral observable properties and in the appearance too are inprinted in the profiles of rotation curves.

b) More specifically small galaxies are fainter and denser, have a steeper rotation curve and more angular momentum per unit of mass and their spiral pattern is less pronounced than large galaxies.

c) Spiral galaxies form with respect to their integral properties a one-parameter sequence being the slope of the rotation curve the best to describe it.

This scenario calls for the constant presence of some amount of dark matter even within the optical disk whose importance varies from galaxy to galaxy.

By means of a model-independent method we obtained the part of the circular velocity due to the self-gravity of the disk eliminating that due to the disk-halo gravitational attraction. So, we found that the dark matter dynamical importance scales inversely proportional to the luminosity. Moreover we are able to theoretically explain the Tully-Fisher relation as the manifestation of centrifugal equilibrium of a self-gravitating disk surrounded by a dark halo and therefore to significantly improve it by taking into account the contribution of dark matter to the equilibrium structure.

In order to obtain disk and halo integral properties we use, after having carefully investigated it, a "minimum of assumptions" model for spiral galaxies. We describe spiral galaxies as two components systems: an exponential thin disk and a dark spherical halo with, at least in a first approximation, a pseudo-isothermal density law with core radius roughly as large as the galaxy size. Then, the ratio of dark matter to visible matter inside the optical size is worked out by means of a method which minimizes the effect of possible uncertainties on the dark matter distribution.

We find that the luminosity sequence is a dark/visible mass ratio sequence being faint galaxies halo dominated (i.e. $M_B = -19$, $H_o = 50$, mass ratio $\simeq 7$), while in luminous galaxies (i.e. $M_B = -22$) the dark mass within the optical radius roughly equals the luminous one.

Moreover, this ratio shapes the profiles of rotation curves. This is a crucial point that strongly demands a dynamical explanation in some stage of the disk formation. In fact we find that the density distributions of visible and dark matter makes rotation curves insensitive to their separate mass distributions but very sensitive to dark/visible mass ratio: in any galaxy at any radius inside the disk, the dark matter distribution is not independent of the visible matter distribution: they act in agreement to make galaxies a one-parameter sequence with relevant parameter the total effective mass distribution or equivalently

the dark/visible mass ratio.

The derived halo properties have been investigated: firstwhole, if the ratio total to luminous mass is a "cosmological" constant $\sim$ 10 , then halo properties range over many orders of magnitudes: in a small galaxy already at the optical radius $M_T/M_H \sim 10$ so that $R_H \sim 5$ kpc; in a large galaxy instead at the optical radius $M_T/M_H \sim 1.5$ so that $R_H \sim 0.5$ Mpc. Then, according to this picture, due to the dissipationless character of halos, we realize that proto-halos were formed with very different mean densities and sizes.

Furthermore, the derived halo mean densities and sizes endow us with their autocorrelation function: we find that it matches remarkably well the galaxy-galaxy correlation function, this both strongly supports the hierarchical clustering picture ($\xi(r)$ is found to have the same slope from the single galaxy to superclusters) and it is the first direct dynamical proof that halos are dissipationless (dissipational dark matter would yield to a much steeper slope for the auto-correlation function).

Then, from the results of this thesis the following picture of disk formation emerges: perturbations of a wide range of length scales formed proto-halos with very different physical properties. Baryonic matter fell in them acquiring its angular momentum and dissipating. This process probably was a dynamical coupling between proto-disk and the halo and the result was different according to the properties of proto-halo. The small et very dense halos prevented baryonic matter from filling completely its potential walls, a large and low density halo allowed baryonic matter to largely fill its potential well, so that disk size is fixed by the astrophysics of the disk formation.

N-body simulations indicate that virialized proto-halo "rotation curves" had smooth slightly rising profile, this is confirmed for the region inside the optical size from the results of this work .This in addittion to some halo-disk dynamical coupling (i.e. the push in effect that the infall of baryonic matter causes on the dark halo suggested by the S. Cruz group

and/or some instability transferring outwards angular momentum.) could explain the "conspiracy" of linear rotation curves.

Of course this picture must be quantitatively checked, but we think that now we have the building blocks (i.e. the physically relevant properties for halos and disks) to allow theories to account for real spiral galaxies.

Let us conclude indicating some observations that ,in our opinion, would be extremely useful and clarifying.

1) Small galaxies seem to be very interesting object; they are completely dominated by the dark halo so that we could investigate even local properties. Nevertheless, there are very few non-local objects in the range -18 ∴ -20 blue magnitude with measured rotation curve. Therefore we suggest a systematic observational effort towards the low luminosity normal spiral galaxies.

2) Quite unbelievingly, more than 1/3 of galaxies with extended high quality rotation curves do not have any photometric observations of color . In detail, the B-V and the B-I is known for 2/3 of the galaxies, the U-B for 1/3 of the galaxies We think that, a great improvement on the direct knowledge of galaxy properties would come from multicolor observations (at the moment less than 20 % of galaxies have U,B,V,R,I colors): when we observe colors we are actually (via evolutionary stellar model) measuring disk masses. Therefore we would like to suggest some project aimed at obtaining multicolor information for a sample of galaxies with known kinematics (i.e. sample B).

BIBLIOGRAPHY

Aaronson, M., Huchra, J., and Mould, J. 1979, A.p.J., 229, 1

Aaronson, M., Huchra, J., and Mould, J., Tully R.B., Fisher, J.R., van Woerden, H.and Goss, W.M., Chamaraux, P., Mebold, U., Siegman, B., Berriman, G., Persson, S.E. 1982, A.p.J.(Suppl. Ser.), 50, 241

Athanassoula, I., 1981 Phys. Rep., 114, 315

Bahcall, J.N. 1986 submitted to Ann. Rev. Astr. Astroph.

Bahcall, J.N., Schmidt, M.,and Soneira R.M. 1983, A.p.J., 265, 730

Bahcall, J.N., and Casertano, S. 1985, A.p.J.(Lett), 300, L35

Barabanov, A.V. and Kyazumov, G.A. 1981, Sov. Astr. Lett.,

Bertin, G., 1980 Phys. Rep., 61,1

Blackman, C.P. 1982, M.N.R.A.S., 184, 397

Blumenthal, G.R., Faber, S.M., Flores, R. and Primack, J.R. 1986, A.p.J., 301, 27

Boroson, T. 1981, A.p.J.(Suppl.) 46, 177

Boroson, T., Strom, K.M. and Strom, S.E. 1983, A.p.J., 274, 39

Bosma, A. 1981, A.J., 86, 1825

Burstein, D. and Rubin, V.C., Thonnard, N., Ford, W.K. 1982 A.p.J, 253, 70

Burstein, D. and Rubin, V.C. 1986 A.p.J., 286, 423

Carignan, C. and Freeman, K.C. 1985, A.p.J., 294, 494

Chincarini, G. and de Sousa, R. 1985, A.A., 153, 218

Compte G. 1984, New Aspects on Galaxy Photometry, Lecture Notes in Physics 232, 170

Dekker, E. 1977, Phys. Rep., 24, 315

Elmegreen, D.M. and Elmegreen, B.G. 1984, A.p.J.(Suppl.), 54, 127

Elmegreen, B.G. and Elmegreen, D.M. 1985, A.p.J., 288, 438

Efstathiou, G., Lake, G. and Negroponte, J. 1982, M.N.R.A.S., 199, 1069

Fall, M.S. 1979, Rev. Mod. Phys., 51, 21

Fall, M.S. and Efstathiou G. 1980, M.N.R.A.S. 193, 189

Freeman, K.C. 1970, A.p.J., 160, 811

Freeman, K.C. 1975, in Galaxies and the Universe, p. 409. The University of Chicago Press, London

Frenk, C.S., White, S.D.M., Efstathiou G., Davis, M. 1985, Nature, 317, 595

Fridman, A.M. and Polyachencko, V.L. 1984, Physics of Gravitating Systems II, p. 168. Springer Verlag, Berlin

Flores, R., Blumenthal, G.R., Dekel, A., Primack, J.R. , SCIPP 86/64 preprint

Gottesman, S.T., Ball, R., Hunter, J.H. and Huntley, J.M. 1984, A.p.J., 286, 471

Grosbol, P.J. 1985, A.A.(Suppl. Ser.) 60, 261

Griersmith, D. 1980, A.J., 85, 1135

Hamabe, M. 1982, Publ. Astron. Soc. Japan, 34, 423

Hoffman, Y. and Shaham, J., A.p.J. 1985, 297, 16

Hegyi, D.J. and Olive, K.A. 1983, Phys. Lett., 126B, 28

Hegyi, D.J. and Olive, K.A. 1986, A.p.J. 303, 56

Karachentchev, I.D. and Mineva V.A. 1980, Sov. Astr. Lett. 10, 105

Kent, S.M. 1984, A.p.J.(Suppl.), 56, 105

Kent, S.M. 1986, A.J., 91, 1301

Kyazumov, G.A. 1984, Sov. Astr., 28, 496

Lindblad, B. 1956, Sthockholm Obs. Ann., Band 17 No 9

Morris, S., Ward, M., Whittle M., Wilson, A.M. and Taylor, K. 1985, M.N.R.A.S., 216, 193

Monet, D.G., Richstone, D.O. and Schechter, P.L. 1981, A.p.J., 245, 454

Persic, M. and Salucci, P. 1986, M.N.R.A.S., in publication

Peterson, C.J. 1978, A.p.J., 226, 75

Quinn, P.J., Salmon, J.K. and Zurek, W.H. 1986, Nature, 322, 329

Richter, O.G. and Huchtmeier W.K. 1984, A.A., 132, 253

Rohlfs, K. 1982, A.A. 105, 296

Romanshin, W. 1983, M.N.R.A.S., 204, 909

Rubin, V.C., Ford W.K. and Thonnard, N. 1980, A.p.J., 238, 471

Rubin, V.C., Ford W.K., Thonnard, N. and Burstein D. 1980, A.p.J., 261, 439

Rubin, V.C.,Burstein, D. Ford W.K. and Thonnard, N. 1980, A.p.J., 289, 81

Schweizer, F., Whitmore, B.C. and Rubin, V.C. 1983

Sanders, R.H. 1984, A.A., 136, L21

Sanders, R.H. 1986, A.A. 154, 135

Sanders, R.H. 1986, preprint ESO

Simien, F. and de Vaucouleurs, G. 1986, A.p.J. 302, 564

Schweizer, F., Rubin, V.C., Whitmore, B.C. 1983, A.J., 88,909

Tinsley, B.M. 1981, M.N.R.A.S. 194, 63

Toomre, A. 1977, Ann. Rev. Astron. Astrophys., 15, 437

Tully, R.B. and Fisher, J.R. 1977, A.A., 54, 661

Vader, P. in Formation and Evolution of Galaxies and Large Structures in the Universe, p. 227, D. Reidel

van Albada, T.S., Bahcall, J.N., Begeman, K. and Sancisi, R. 1985, A.p.J., 295, 305

van Albada, T.S. and Sancisi R. 1986, Phil. Trans. R. Soc. Lond. (in press)

van der Kruit, P.C. and Searle, L. 1982, A.A., 110, 61

van der Kruit, P.C. 1986, submitted to A.A.

van Moorsel, G.A. 1982, A.A. 107, 66

van Moorsel, G.A. 1984, A.A.(Suppl. Series), 53, 19

van Moorsel, G.A. 1984, A.A.(Suppl. Series), 54, 1

van Moorsel, G.A. 1984, A.A.(Suppl. Series), 54, 19

Vivanathan, N. and Griersmith, D. 1979, A.p.J., 230, 1

Tully, R.B., Mould, J.R. and Aaronson, M. 1982, A.p.J., 257, 527

Whitmore, C.W., McElroy, D.B. and Schweizer 1986, preprint

Wyse, F.G. 1982, M.N.R.A.S., 199, 1P

Rubin, V.C., Ford W.K. and Thonnard, N. 1980, A.p.J., 238, 471

Rubin, V.C., Ford W.K., Thonnard, N. and Burstein D. 1980, A.p.J., 261, 439

Rubin, V.C.,Burstein, D. Ford W.K. and Thonnard, N. 1980, A.p.J., 289, 81

Schweizer, F., Whitmore, B.C. and Rubin, V.C. 1983

Sanders, R.H. 1984, A.A., 136, L21

Sanders, R.H. 1986, A.A. 154, 135

Sanders, R.H. 1986, preprint ESO

Simien, F. and de Vaucouleurs, G. 1986, A.p.J. 302, 564

Schweizer, F., Rubin, V.C., Whitmore, B.C. 1983, A.J., 88,909

Tinsley, B.M. 1981, M.N.R.A.S. 194, 63

Toomre, A. 1977, Ann. Rev. Astron. Astrophys., 15, 437

Tully, R.B. and Fisher, J.R. 1977, A.A., 54, 661

Vader, P. in Formation and Evolution of Galaxies and Large Structures in the Universe, p. 227, D. Reidel

van Albada, T.S., Bahcall, J.N., Begeman, K. and Sancisi, R. 1985, A.p.J., 295, 305

van Albada, T.S. and Sancisi R. 1986, Phil. Trans. R. Soc. Lond. (in press)

van der Kruit, P.C. and Searle, L. 1982, A.A., 110, 61